

Please cite this paper as : C. Lupan, N. Wolff, J. Drewes, H. Krüger, A. Vahl, T. Pauporté, O. Lupan, B. Viana, L. Kienle, F. Faupel, R. Adelung, S. Hansen, Nanosensors Based on a Single ZnO:Eu Nanowire for Hydrogen Gas Sensing. ACS Appl. Mater. Interfaces, 14 (2022) 41196–41207. DOI: 10.1021/acsami.2c10975

Nanosensors Based on a Single ZnO:Eu Nanowire for Hydrogen Gas Sensing

Cristian Lupan,^{1,*} Abhishek Kumar Mishra,^{2,*} Niklas Wolff,³ Jonas Drewes,⁴ Helge Krüger,⁵

Alexander Vahl,^{4,*} Oleg Lupan,^{1,5,6,7,*} Thierry Pauporté,⁶ Bruno Viana,⁶ Lorenz Kienle,³

Rainer Adelung,⁵ Nora H de Leeuw,^{8,9} Sandra Hansen,^{5,*}

¹ Center for Nanotechnology and Nanosensors, Department of Microelectronics and Biomedical Engineering, Faculty of Computers, Informatics and Microelectronics, Technical University of Moldova, 168 Stefan cel Mare str., MD-2004, Chisinau, Republic of Moldova

² Department of Physics, Applied Science Cluster, School of Engineering, University of Petroleum and Energy Studies (UPES), Energy Acres Building, Bidholi, Dehradun 248007, Uttarakhand, India

³ Chair for Synthesis and Real Structure, Faculty of Engineering, Department of Materials Science, Kiel University, Kaiserstr. 2, D-24143, Kiel, Germany

⁴ Chair for Multicomponent Materials, Faculty of Engineering, Department of Materials Science, Kiel University, Kaiserstr. 2, D-24143, Kiel, Germany

⁵ Functional Nanomaterials, Faculty of Engineering, Department of Materials Science, Kiel University, Kaiserstr. 2, D-24143, Kiel, Germany

⁶ PSL Université, Chimie ParisTech, CNRS, Institut de Recherche de Chimie Paris (IRCP), 11 rue P. et M. Curie, F, 75005 Paris, France

⁷ Department of Physics, University of Central Florida, Florida, Orlando, FL 32816-2385, USA

⁸ School of Chemistry, University of Leeds, Leeds LS2 9JT, United Kingdom

⁹ Department of Earth Sciences, Utrecht University, Princetonlaan 8a, 3584 CB Utrecht, The Netherlands

*Corresponding authors:

C. Lupan (cristian.lupan@mib.utm.md)
Technical University of Moldova, Republic of Moldova

Prof. Dr. Abhishek Kumar Mishra (akmishra@ddn.upes.ac.in)
University of Petroleum and Energy Studies (UPES), Dehradun

Dr. Alexander Vahl (alva@tf.uni-kiel.de)
Kiel University, Germany

Dr. S. Hansen, (sn@tf.uni-kiel.de)
Kiel University, Germany

Prof. Dr. O. Lupan, (ollu@tf.uni-kiel.de ; oleg.lupan@mib.utm.md)
Kiel University, Germany; Technical University of Moldova, Moldova; UCF, U.S.A.

Please cite this paper as : C. Lupan, N. Wolff, J. Drewes, H. Krüger, A. Vahl, T. Pauporté, O. Lupan, B. Viana, L. Kienle, F. Faupel, R. Adelung, S. Hansen, Nanosensors Based on a Single ZnO:Eu Nanowire for Hydrogen Gas Sensing. ACS Appl. Mater. Interfaces, 14 (2022) 41196–41207. DOI: 10.1021/acsami.2c10975

KEYWORDS: Eu_2O_3 , ZnO, sensor, hydrogen, electrochemical deposition.

ABSTRACT

Fast detection of hydrogen gas leakage or its release in different environments, especially in large electric vehicle batteries, is a major challenge for sensing applications. In this study, the morphological, structural, chemical, optical and electronic characterization of ZnO:Eu nanowire arrays is reported and discussed in detail. In particular, the influence of different Eu concentrations during electrochemical deposition was investigated together with the sensing properties and mechanism. Surprisingly, by using only 10 μM Eu ions during deposition, the value of the gas response increased by a factor of nearly 130 compared to an undoped ZnO nanowire and we found an H_2 gas response of ~ 7860 for a single ZnO:Eu nanowire device. Further, the synthesized nanowire sensors were tested with ultraviolet (UV) light and a range of test gases, showing a UV responsiveness of ~ 12.8 and a good selectivity to 100 ppm H_2 gas. It is demonstrated dual-mode nanosensor to detect UV/ H_2 gas simultaneously for selective detection of H_2 during UV irradiation and effect on sensing mechanism. The nanowire sensing approach here demonstrates the feasibility of using such small devices to detect hydrogen leaks in harsh, small-scale environments, for example stacked battery packs in mobile applications. In addition, the results obtained are supported through Density Functional theory-based simulations, which highlight the importance of rare earth nanoparticles on the oxide surface for improved sensitivity and selectivity of gas sensors, even at room temperature, thereby allowing, for instance, lower power consumption and denser deployment.

1. INTRODUCTION

Hydrogen (H_2) is an extremely useful gas that has great potential for future applications as it represents an alternative, clean, sustainable and promising energy source for the stationary and transportation sectors ^{1,2}. However, hydrogen gas is also a common decomposition product of chemical reactions such as those that occur during battery operation, and therefore must be detected, owing primarily to its reactivity and hazardousness ³⁻⁵. In batteries, especially in large vehicle applications, several types of defects can increase the temperature and lead to undesirable chemical reactions that can also cause thermal runaway ⁶⁻⁸. Any fault condition must be investigated and preferably prevented during operation to increase safety, as health hazards such as toxic (e.g. CO, HF) and flammable (e.g. H_2 , CH_4 , C_2H_4 , electrolytes) gases, as well as fire and explosions may occur ^{6,7}. Therefore, several research groups are investigating the gas evolution, especially of H_2 and CO,

Please cite this paper as : C. Lupan, N. Wolff, J. Drewes, H. Krüger, A. Vahl, T. Pauporté, O. Lupan, B. Viana, L. Kienle, F. Faupel, R. Adelung, S. Hansen, Nanosensors Based on a Single ZnO:Eu Nanowire for Hydrogen Gas Sensing. ACS Appl. Mater. Interfaces, 14 (2022) 41196–41207. DOI: 10.1021/acsami.2c10975 in different types of battery cells during overcharging and at high temperatures to enable the development of appropriate early warning systems. Such systems are based on new materials and are in particular relevant for detection of H₂ levels during over-temperature triggering to avoid various hazards^{4,9,10}. Another major safety issue with H₂ is its ability to diffuse very easily and mix quickly with the air by diffusion. The International Fire Code (IFC) allows H₂ levels as high as 1% vol¹¹, while mixing ratios of hydrogen with oxygen ranging above 4% (Lower Explosive Limit (LEL) or the Lower Flammability Limit (LFL)) and below 75% (Upper Explosive Limit (UEL) or the Upper Flammability Limit (UFL)) by volume are highly explosive and therefore dangerous¹². Since both the hydrogen-oxygen mixture flame and combustion flames emit UV radiation, which is invisible to the human eye, a device containing, an H₂ gas sensor and a UV detector as dual-mode sensor or two separate devices, are required for safety monitoring and raising the alarm¹³. With the increasing use of hydrogen and the demand for small, cheap and new electronic devices that can detect hazardous gases, semiconductor oxide-based multifunctional devices are one of the most relevant types for future sensing applications owing to their small size, improved safety, usually good and direct sensing response, and increased efficiency¹⁴. Micro- and nanodevices based on new functional oxides are now the focus of applied research, as they are expected to become the largest and fastest market, with sales exceeding trillions of euros¹³.

Zinc oxide (ZnO) is a semiconductor oxide material that is often used in sensing applications, but it suffers from poor selectivity, high operating temperature and inadequate response. However, mixing or doping with impurities^{14,15} and surface functionalization with rare earth elements, such as Ce, Eu, Er^{16–18} improves the sensing properties, due to catalytic efficiency and access to oxygen ions and the high basicity of the ZnO surface^{15,19}. However, technologies are needed to synthesize such a combination of oxides with rare earth elements that can be used on a larger scale. In addition, Eu³⁺ ions improve the photocatalytic properties of ZnO by reducing the recombination of electron-hole pairs²⁰, after creating an energy level of impurities that improves the absorption properties of the material²¹. By doping ZnO with rare earth elements^{15,21}, mixing and/or and surface functionalization with noble metal nanoparticles, a better response and lower operating temperature have already been observed for gas sensing applications^{16–18}.

ZnO doped or mixed with rare earth elements (Tb, Eu, Ce, Er, La, etc.) for sensing applications have been studied by several groups to increase the response value, control selectivity and to reduce the operating temperature^{15,22,23}. Zhao et al.²² reported the effects of doping rare earth

Please cite this paper as : C. Lupan, N. Wolff, J. Drewes, H. Krüger, A. Vahl, T. Pauporté, O. Lupan, B. Viana, L. Kienle, F. Faupel, R. Adelung, S. Hansen, Nanosensors Based on a Single ZnO:Eu Nanowire for Hydrogen Gas Sensing. ACS Appl. Mater. Interfaces, 14 (2022) 41196–41207. DOI: 10.1021/acsami.2c10975

elements in ZnO nanowires (NWs) on the sensing performances and found that ZnO NWs doped with 1% Ce responded best to ethanol. Hastir et al.¹⁵ investigated the gas sensor properties by doping ZnO with Tb, Dy and Er, observing significant improvement in the sensitivity to ethanol and a decrease in the operating temperature. Also, by doping ZnO with Tb and Er, a selectivity to ethanol and acetone was observed¹⁵. Here, the improvement in gas sensor response was attributed to changes caused by rare earth doping, such as high surface basicity, increased surface area, morphological changes and the presence of oxygen vacancies¹⁵. A reduction in the optimum operating temperature due to doping was explained by catalytic effects which increase the reaction rate, as well as provide various reaction pathways that possess lower activation energies towards the applied gas^{15,23}. Rare earth elements, such as europium and its oxides, can enhance the sensing properties of zinc oxide due to catalytic efficiency, high mobility of oxygen ions and basicity of the surface. However, to our knowledge, there are no reports so far of H₂ detectors or UV/H₂ dual-mode nanosensors made from such a combination of oxides.

Nano-sensors, micro-sensors based on Eu-doped/functionalized zinc oxide is considered to have advantages such as lower operating temperature (down to room temperature) to eliminate potential drawbacks due to heat exposure, a lower device cost, and lower power consumption. In addition, nano-sensors offer the important advantage that their small size allows them to be integrated into various devices to monitor and detect hazardous gases in multiple places on larger batteries, such as in vehicles, which is clearly a motivation for further research.

In this work, ZnO:Eu nanowire arrays were fabricated by an electrochemical deposition method and integrated into nano-sensors as individual nanowires. Next, the morphological, chemical, structural, optical and sensor properties of different concentrations of Eu in ZnO:Eu composites were investigated. The potential nano-sensors for the detection of UV light and hydrogen gas detection was also evaluated for ZnO:Eu nanowire-based devices and dual-mode sensor. Density Functional Theory (DFT) based simulations have provided insights into Eu doping-mediated H₂ gas sensing on ZnO nanowires.

2. EXPERIMENTAL AND COMPUTATIONAL DETAILS

ZnO:Eu nanowire-networks were grown onto Fluor-Tin Oxide (FTO) films on glass substrates using an electrochemical deposition method^{21,24} by mixing 0.02 M ZnCl₂ and 1 M KCl as precursors and different concentrations of EuCl₃ (3, 5, 6, 7, 8, 9, 10, 20 μM) for mixing or surface

Please cite this paper as : C. Lupan, N. Wolff, J. Drewes, H. Krüger, A. Vahl, T. Pauporté, O. Lupan, B. Viana, L. Kienle, F. Faupel, R. Adelung, S. Hansen, Nanosensors Based on a Single ZnO:Eu Nanowire for Hydrogen Gas Sensing. *ACS Appl. Mater. Interfaces*, 14 (2022) 41196–41207. DOI: 10.1021/acsami.2c10975 deposited with Eu³⁺ ions in deionized water with a resistivity of 18.2 MΩ·cm. Samples were noted as Eu3 for 3 μM, Eu6 for 6 μM and Eu10 for 10 μM EuCl₃ in the electrolyte, respectively.

Different sets of ZnO:Eu nanowire-networks were investigated by X-ray photoelectron spectroscopy (XPS, Omicron Nano-Technology GmbH, Al-anode, 240W), to determine the chemical/electronic properties. The measured spectra were referenced towards the C-1s line of aliphatic carbon at 285.0 eV²⁵. CasaXPS (version 2.3.16) was used for this purpose. SEM, XRD and microRaman studies were conducted as previously reported^{23,26}. The WITec micro-Raman spectrometer was used in this study, and a 532-nm laser served as the excitation source. A monochromator with a 1200 groove·mm⁻¹ grating was used to disperse the scattered light, afterwards focused onto a charge-coupled detector (CCD, Wright Instruments, Ltd.). Before all investigations, this equipment was calibrated using a Si wafer.

For transmission electron microscopy (TEM) investigation, the functionalized ZnO:Eu nanowires were scratched from the Fluor-Tin Oxide (FTO) substrate onto a lacey-carbon copper grid. The structural and chemical investigation were performed on a FEI Tecnai F30 microscope. Energy-dispersive X-Ray spectroscopy (EDS) was enabled using an EDAX Si-Li drift detector for chemical species identification and elemental mapping. In addition, the energy-filtered (EF)TEM technique was applied for elemental imaging of europium species using the Eu(N)-edge at 143 eV. Electron energy-loss spectroscopy (EELS) was involved in the determination of the Eu oxidation state by collecting the energy-loss signals of the N_{4,5}-edge at 143 eV and M_{4,5}-edge around 1130 eV, respectively. Background subtraction was performed using the EELS plug-in implemented in the *DigitalMicrograph* software. The individual spectra were adjusted by an energy shift according to the shift of the zero-loss peak (ZLP) acquired before each measurement. The spectra were recorded with an energy resolution of 1.8 eV (half-width of the ZLP).

Samples with different europium content were prepared by an electrochemical growth process at 80 °C, and micro-nanodevices were prepared by maskless nanoscale deposition in the focused electron/ion beam instrument (FEI, Helios Nanolab). In particular, a single ZnO:Eu nanowire was integrated into a device with two prepatterned electrodes, Si/SiO₂ and quartz with Cr/Au pads as contact electrodes, as previously reported^{27,28}. The study of the electrical current of a nanosensor based on a single ZnO:Eu nanowire was investigated using a two-point probe. By controlling the electrical current in the developed device, the electrical conductivity was studied in the environment and by exposing the nanosensor to a test gas. The nanosensors were tested at operating temperatures

Please cite this paper as : C. Lupan, N. Wolff, J. Drewes, H. Krüger, A. Vahl, T. Pauporté, O. Lupan, B. Viana, L. Kienle, F. Faupel, R. Adelung, S. Hansen, Nanosensors Based on a Single ZnO:Eu Nanowire for Hydrogen Gas Sensing. ACS Appl. Mater. Interfaces, 14 (2022) 41196–41207. DOI: 10.1021/acsami.2c10975 ranging from room temperature (RT) to 175 °C to observe the effect of this parameter on UV and gas detection performances. All nanosensors were tested at a relative humidity of 10% in the test chamber, and the effect of humidity was investigated by raising the humidity to 50% RH. Nanosensors ZnO:Eu₃ were tested in dual-mode to see clearly detection of H₂ gas during continuous UV light pulse.

We have performed DFT simulations, employing the generalized gradient approximation (GGA) within the PBE-Perdew–Burke–Ernzerhof²⁹ exchange–correlation functional and the projected augmented wave (PAW) approach^{30,31}, as implemented in the Vienna *ab initio* Simulation Package (VASP)³². We have used the ZnO bulk and subsequent surface structures from previous work^{27,33,34} as a starting model to investigate gas sensing, where the ZnO bulk unit cell structure was optimized using a 5×5×4 Monkhorst-Pack *k* point mesh³⁵. The 4×4 supercell of the ZnO (10 $\bar{1}$ 0) surfaces was modelled using a 3×3×1 Monkhorst-Pack *k* point mesh. The DFT-D3 approach as described by Grimme³⁶ and implemented in VASP was employed to incorporate the long-range dispersion corrections while investigating gas molecule interactions. Other details remain the same as described in our earlier works^{27,33,34}.

The adsorption energy of the H₂ molecule was computed as follows:

$$E_{\text{ads}} = E_{\text{Complex}} - (E_{\text{Surf}} + E_{\text{Mol}}) \quad (1)$$

where E_{Complex} is the total energy of the surface with the molecule, E_{Surf} is the energy of the surface slab without the molecule, and E_{Mol} is the energy of the isolated molecule. E_{Mol} was calculated by modeling the isolated molecule in the center of a broken symmetry cell with lattice constants of 20 Å, inspecting only the Gamma point of the Brillouin zone with the same accuracy parameters as employed for the surface's structures. Bader charges were calculated using the method developed by Henkelman and co-workers³⁷.

3. RESULTS AND DISCUSSION

3.1. Morphological and structural characteristics

Figure 1 presents SEM images at different magnifications showing the morphology of the synthesized ZnO:Eu nanowire arrays, namely ZnO:Eu₃, ZnO:Eu₅ and ZnO:Eu₁₀ sample sets. The low magnification images (**Figure 1a, 1d, 1g**) indicate a complete and homogeneous coverage of the

Please cite this paper as : C. Lupan, N. Wolff, J. Drewes, H. Krüger, A. Vahl, T. Pauporté, O. Lupan, B. Viana, L. Kienle, F. Faupel, R. Adelung, S. Hansen, Nanosensors Based on a Single ZnO:Eu Nanowire for Hydrogen Gas Sensing. ACS Appl. Mater. Interfaces, 14 (2022) 41196–41207. DOI: 10.1021/acsami.2c10975

FTO substrate by nanowire arrays, which exhibit highly uniform wires with even distribution in length and diameter, as evidenced by the high magnification images (**Figure 1b, 1e, 1h**). There are no significant differences in the nanowire morphologies with respect to the increased concentration of EuCl₃ in the deposition electrolyte (**Figure 1c, 1f, 1i**). Individual nanowires were then incorporated into the nanosensor device using a FIB-SEM technique described in previous works^{38,39}. Each nanowire was connected to contact pad Au electrodes by the deposition of a Pt line from a Pt-containing precursor using the metallic maskless deposition in a focused electron/ion beam system. The selected nanowires possess comparable high aspect ratios with a diameter of ~ 90 nm and lengths of ~ 1.6 μm (see **Figure 7a**).

The crystal structure and crystal orientation of the ZnO:Eu nanowire arrays grown on the FTO/glass substrates were investigated by X-ray diffraction (XRD). **Figure 2** shows the XRD patterns of ZnO:Eu6 and ZnO:Eu10. The reflections of the ZnO lattice can be indexed to the hexagonal wurtzite-type structure according to the standard card (PDF 036-1451). One single Eu₂O₃ reflection peak was detected at 42.47° for ZnO:Eu6 and ZnO:Eu10, attributed to the cubic phase, according to PDF 03-065-3182. FTO substrate reflections have been attributed and are marked with the red circle in **Figure 2**. The nanowires are preferentially oriented along the *c*-axis direction, shown by the high-intensity reflection at 34.42° for the (0 0 0 2) plane of ZnO. Further, the good signal to noise ratio of the ZnO reflections indicate high crystallinity of the samples²⁴.

TEM measurements (see **Figure 3** and **Figure S1**) on the ZnO:Eu10 nanowires (10 μM) show uniform dimensions with lengths of 1.5 - 2 μm and diameters of 150 - 300 nm. Their crystalline structure was determined by high-resolution (HRTEM) imaging and electron diffraction (see **Figure 3, Figure 3b** and **Figure S1**). HRTEM imaging further evidences a network of dominantly amorphous particles which partially covers the nanowires. Spectroscopic analysis on these agglomerates using EDS (see **Figure S1**) and EFTEM imaging (see **Figure 3c**) reveals Eu-containing species, associated with further content of silicon from the substrate and oxygen.

The valence state of Eu in the agglomerates is determined by analysis of the characteristic energy-losses of the inelastic scattered transmitted electrons⁴⁰⁻⁴³. The oxidation states of Eu²⁺ and Eu³⁺ are distinguishable either by a 2.5 eV energy shift of the characteristic N₅ and M₅ main core-loss features located at 143 eV and 1131 eV or by the shape of the N_{4,5}-edge featuring a double peak in the case of Eu³⁺ ions.

Please cite this paper as : C. Lupan, N. Wolff, J. Drewes, H. Krüger, A. Vahl, T. Pauporté, O. Lupan, B. Viana, L. Kienle, F. Faupel, R. Adelung, S. Hansen, Nanosensors Based on a Single ZnO:Eu Nanowire for Hydrogen Gas Sensing. ACS Appl. Mater. Interfaces, 14 (2022) 41196–41207. DOI: 10.1021/acsami.2c10975

The EELS fine structure analysis is presented in **Figures 3d** and **3e** showing the distinct fingerprints of the $N_{4,5}$ - and $M_{4,5}$ -edges in comparison with reference spectra recorded for Eu^{3+} in Eu_2O_3 and a change of valence in interface layers of $\text{EuO}|\text{Si}$ systems, reported previously in Reference ⁴², lines marked as Eu^{3+} . Two representative measurements with STEM EELS identify the spectral signatures of Eu^{3+} at energy-loss features of 143.6 eV and 1136 eV. The deviation on the energy scale of 0.6 eV and 5 eV with respect to the reference values are rationalized by the position instability of the ZLP during the measurement.

In summary, analytical TEM studies reveal the surface functionalization or surface deposited of ZnO nanowires with amorphous networks containing Eu^{3+} ions and provide evidence for the formation of Eu_2O_3 in these agglomerates. Shallow doping of the ZnO lattice with Eu^{3+} during growth was not possible to determine either by superposition of signals from the agglomerates or the limited resolution of the spectroscopic methods to reliably trace element concentrations below 2 at%.

3.2. Chemical properties

To further investigate the possibility of Eu mixing and the Eu content or concentration, XPS measurements were performed for chemical identification, to determine the molecular formula, chemical state, and electronic state of the elements present in a sample. The overview spectrum of the ZnO:Eu nanowire arrays is shown in **Figure 4a** and indicates the presence of Zn, Eu, O and C, as well as Sn (in case of sample ZnO:Eu3, ZnO:Eu6, ZnO:Eu10). The signal of C originates from residual amounts of adventitious carbon, and surface adsorbates such as atmospheric carbohydrates ^{44,45}. The presence of Sn is due to the use of FTO glass as substrate material for electrodeposition. For a detailed comparison, the C-1s, Zn-2p_{3/2} and Eu-3d_{5/2} lines are shown in **Figure 4b**. The different level of mixing in the different samples reflects on the europium signal, or content/concentration level. Accordingly, the corresponding Eu-3d_{5/2} line is the strongest for the ZnO:Eu10 sample and the lowest for the ZnO:Eu3 sample. The position of the Eu-3d_{5/2} line is centred around 1135.6 eV, which corresponds well with Eu^{3+} in Eu_2O_3 ⁴⁶. To indicate the europium concentration level, an exemplary quantification was conducted for the ZnO:Eu10 sample. The quantification of the ZnO:Eu nanowire arrays was performed based on the Zn-2p_{3/2} and Eu-3d_{5/2} lines (**Figure 4b**) for the sample with 10 μM , which showed the highest Eu signal. The Eu/Zn ratio in this XPS spectra quantification is 4/96, which relates to a concentration of europium of roughly 4%.

Please cite this paper as : C. Lupan, N. Wolff, J. Drewes, H. Krüger, A. Vahl, T. Pauporté, O. Lupan, B. Viana, L. Kienle, F. Faupel, R. Adelung, S. Hansen, Nanosensors Based on a Single ZnO:Eu Nanowire for Hydrogen Gas Sensing. ACS Appl. Mater. Interfaces, 14 (2022) 41196–41207. DOI: 10.1021/acsami.2c10975

3.3 Raman

Micro-Raman spectroscopy provides detailed structural data on the electrodeposited material, especially on the nanowire arrays vibrational properties, material quality, and phase. These are important to understand the transport properties and phonon interaction with the free charge carriers to determine the nanodevice performance. Several spectra of samples and different locations on the FTO substrate were measured observing no significant difference. A typical spectrum corresponding to one position on the ZnO:Eu nanowire array is presented. The micro-Raman spectra of two samples with different Eu content (ZnO:Eu8 and ZnO:Eu10) are illustrated in **Figure 5a**. Peaks of the FTO layer at 633 cm^{-1} were found in all samples. All other micro-Raman modes agree with the results for ZnO. The Raman modes for such material can be represented as follows $\Gamma_{opt} = 1A_1 + 2B_1 + 1E_1 + 2E_2$. The mode at the 100 cm^{-1} (E_2 -low) is attributed to the vibration of Zn sub-lattice, while the peak at the 438 cm^{-1} (E_2 -high) is related to the vibration of the oxygen atoms⁴⁷. E_2 -high is attributed to the ZnO nonpolar optical phonons of E_{2H} mode, which is one of the characteristic peaks of wurtzite ZnO with good-quality crystals⁴⁷. A more detailed discussion can be found in a previous work²⁴. Thus, the microRaman spectroscopy study confirms the good crystalline quality of the nanowires observed in the XRD diffractogram.

3.4 Optical properties

The optical properties of ZnO:Eu nanowire arrays with different concentrations of Eu were studied in the wavelength 300 - 1700 nm. The results are shown in **Figure 5b**, where optical transmittance values for ZnO:Eu6, ZnO:Eu8 and ZnO:Eu10 are shown in percentage values from reference sample. A decrease in optical transmission was observed with the increase in Eu content, as reported before²³. It was observed that in the visible spectrum optical transmission values are higher than 65%, while in near-infrared spectrum they are about 85%.

By extrapolating linear segment of $(\alpha h\nu)^2$ versus photon energy ($h\nu$), represented in **Figure 5c**, the optical band gap of ZnO:Eu nanowire arrays with different Eu content was studied. A slight increase was observed with the increase in Eu content, from 3.26 eV for ZnO:Eu6 to 3.27 eV for ZnO:Eu10. These results show that the Eu content in ZnO does not affect significantly the optical band value, which was also observed in other studies²³.

Please cite this paper as : C. Lupan, N. Wolff, J. Drewes, H. Krüger, A. Vahl, T. Pauporté, O. Lupan, B. Viana, L. Kienle, F. Faupel, R. Adelung, S. Hansen, Nanosensors Based on a Single ZnO:Eu Nanowire for Hydrogen Gas Sensing. ACS Appl. Mater. Interfaces, 14 (2022) 41196–41207. DOI: 10.1021/acsami.2c10975

3.5 Gas sensing properties

To determine the response, selectivity and behavior of a single nanowire ZnO:Eu compared to reference ZnO, the electrical response was recorded for different samples and the sensor was inserted into a measurement device. The electrical properties of the single ZnO:Eu nanowire have a significant effect on the response of the gas sensor to H₂ gas. The measurements were performed in the temperature range between 20 and 175 °C. The gas sensor properties of the ZnO:Eu based sensors are investigated under the influence of different test gases, such as acetone, 2-butanol, ethanol, hydrogen, ammonia, *n*-propanol and methane. Here, the gas response (S_g) to the target gas was determined using the ratio of electrical current through the sensor at gas exposure (I_{gas}) and I_{air} represents electrical current in air exposure.

$$S_g = \frac{I_{gas}}{I_{air}} \quad (2),$$

The dynamic response to 100 ppm H₂ gas at room temperature (RT) is represented in **Figure 6a**, showing a gas response of only $S_g = 2.1$ for the sample prepared with 5 μM europium chloride in bath (ZnO:Eu5). The response time represents the time it takes for the sensor to reach 90% of the maximum current after gas exposure. The recovery time represents the time it takes for the sensor to reach 10% of the initial current after stopping the gas exposure. The sample tested demonstrated reasonable response and recovery times, at ~7 s and ~42 s, respectively.

Table 1. Comparison of response value of hydrogen gas sensor using zinc oxide and doped/mixed zinc oxide nanostructures

Study	Nanostructure	Operating temperature	Hydrogen concentration (ppm)	Response value (S_g)
This work	ZnO:Eu5 nanowire	RT	100	2.1
This work	ZnO:Eu20 nanowire	100 °C	100	865
This work	ZnO:Eu20 nanowire	125 °C	100	672

Please cite this paper as : C. Lupan, N. Wolff, J. Drewes, H. Krüger, A. Vahl, T. Pauporté, O. Lupan, B. Viana, L. Kienle, F. Faupel, R. Adelung, S. Hansen, Nanosensors Based on a Single ZnO:Eu Nanowire for Hydrogen Gas Sensing. ACS Appl. Mater. Interfaces, 14 (2022) 41196–41207. DOI: 10.1021/acsami.2c10975

This work	ZnO:Eu10 nanowire	150 °C	100	7860
This work	ZnO:Eu6 nanowire	175 °C	100	1607
Lupan et al. ²³	Pd-functionalized ZnO:Eu films	250 °C	100	115
Rashid et al. ⁴⁸	ZnO nanorod decorated with Pd nanoparticles	RT	1000	1.9
Kohlmann et al. ²⁶	ZnO nanobrush	100 °C	100	25
Kohlmann et al. ²⁶	ZnO nanobrush	125 °C	100	62
Kohlmann et al. ²⁶	ZnO nanobrush	150 °C	100	148
Khan et al. ⁴⁹	ZnO single nanowire	200 °C	100	2.5
Khan et al. ⁴⁹	ZnO multiple nanowires	200 °C	100	5.3

In addition, the sensor showed selectivity to hydrogen gas at room temperature with a response of 2.1 (**Figure 6b**) for the ZnO:Eu5 sample.

In **Table 1** are compared hydrogen gas response for sensors based on ZnO and doped/mixed ZnO, observing that by using ZnO:Eu nanowire – based nanosensors, we obtained a higher response at room temperature for a lower concentration of hydrogen (100 ppm) compared to a previously reported sensor based on Pd nanoparticles decorated on ZnO nanorods with a gas response of $S_g = 1.9$ for 1000 ppm hydrogen at room temperature ⁴⁸.

In addition, a proof-of-concept study measured the dynamic response of the sensor current to UV light at room temperature, and the properties upon UV light irradiation are shown in **Figure S2a** for ZnO:Eu5 sample set. Here, a response time of ~28 s and ~10 s for the recovery time were observed. The response time to UV is higher than to hydrogen, while it recovers faster from UV exposure back to the baseline. Long response times to UV light can be explained by a gradual accumulation of unpaired electrons on the nano-sensor surface until desorption and re-adsorption of oxygen reach an equilibrium state ⁵⁰. The recovery time is caused by the quick recombination of holes with electrons when the UV light is switched off ⁵⁰.

The UV response (S_{UV}) was determined using the ratio:

Please cite this paper as : C. Lupan, N. Wolff, J. Drewes, H. Krüger, A. Vahl, T. Pauporté, O. Lupan, B. Viana, L. Kienle, F. Faupel, R. Adelung, S. Hansen, Nanosensors Based on a Single ZnO:Eu Nanowire for Hydrogen Gas Sensing. ACS Appl. Mater. Interfaces, 14 (2022) 41196–41207. DOI: 10.1021/acsami.2c10975

$$S_{UV} = \frac{I_{UV}}{I_{dark}} \quad (3),$$

where I_{UV} is an electrical current through sensor at UV light exposure and I_{dark} represents electrical current without UV light exposure.

The dynamic response to UV light at an operating temperature of 100 °C is shown in **Figure 6c**, where sensor ZnO:Eu5 showed a higher response than at room temperature to UV light of ~12.8, with faster response and recovery times of ~8 s and ~7 s, respectively.

In **Figure 7c** and **Figure S3** the gas response to a series of different gases are shown and compared. From operating temperatures of 100 °C to 175 °C a response and selectivity to 100 ppm hydrogen gas for all mixing concentrations of Eu was observed. All samples showed a gas response starting at 100 °C, increasing with increasing temperature up to 150 °C, and then decreasing, except for the ZnO:Eu6 sample (see **Figure S3a**). The maximum response of ~7860 was achieved at 150 °C for the ZnO:Eu10 sample (see **Figure 7b**), dropping to ~675 at 175 °C. The response time for the ZnO:Eu10 nanosensor at 150 °C was ~17 s, while the recovery time was less than half a second.

ZnO:Eu3 nanosensor was exposed to UV light and hydrogen gas at the same time to observe the influence on the sensing performance as a dual-mode sensor. In **Figure S2b**, nanosensor was exposed continuously for ~27 seconds to 100 ppm hydrogen gas and only for ~10 seconds to UV light simultaneously. It was observed that hydrogen response value of ~44 was not influenced by the UV light applied in the middle of H₂ gas pulse.

However, in **Figure S2c**, nanosensor ZnO:Eu3 was exposed continuously for ~26 seconds to UV light and only for ~10 seconds to 100 ppm hydrogen. It was observed that after applying hydrogen gas, response value increased from ~11 to ~28, marked in the middle of the pulses overlapping, in **Figure S2c**. After stopping hydrogen gas, response value decreased to ~13, which is almost same value obtained under UV irradiation. Thus, we demonstrated dual-mode nanosensor to detect UV/H₂ light/gas simultaneously for selective detection of H₂ gas during UV irradiation and contribute to study its effect on sensing mechanism.

These results can be explained by the fact that nanosensor has higher response value to hydrogen gas of ~48 for this doping concentration, while the one for UV light is lower, meaning that during UV light exposure response value is influenced by the hydrogen gas, until it reaches saturation.

When ZnO:Eu nanowires are exposed to UV light, photogenerated electron-hole pairs are created, affecting the chemisorption and desorption processes that take place on the surface of the nanosensor during hydrogen gas exposure⁵¹. However, applying H₂ gas pulse in the middle or

Please cite this paper as : C. Lupan, N. Wolff, J. Drewes, H. Krüger, A. Vahl, T. Pauporté, O. Lupan, B. Viana, L. Kienle, F. Faupel, R. Adelung, S. Hansen, Nanosensors Based on a Single ZnO:Eu Nanowire for Hydrogen Gas Sensing. ACS Appl. Mater. Interfaces, 14 (2022) 41196–41207. DOI: 10.1021/acsami.2c10975

simultaneously with an UV light, it can suggest that hydrogen interacts with adsorbed oxygen species on the surface of ZnO:Eu. Thus, it contributes to sensing mechanism and to development of dual-mode nanosensor. It was selected this concentration ZnO:Eu₃, because for it was more clearly observed this effect and response values are comparable.

Figure 8 shows a comparison of hydrogen gas response values at operating temperature of 150 °C for ZnO:Eu samples with different Eu content. It was observed that the response value increased with the increase in Eu content in the samples, from ~60 for the undoped ZnO:Eu₀ up to ~7860 for surface deposited ZnO:Eu₁₀, then decreased to ~3725 for ZnO:Eu₂₀. These results can be explained by the energy difference needed for activation, meaning that samples with different Eu content and operating temperature, directly influence the sensor properties.

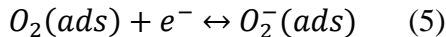
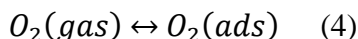
To verify the stability and repeatability of the ZnO:Eu₂₀ nanosensor at 100 ppm hydrogen gas, a nano-sensor was tested after 10 months, with the results shown in **Figure S4**. Initially, the maximum response value was ~3725 at 150 °C, but after 10 months, the response value decreased to ~900 at the same operating temperature. In contrast, it was observed that after 10 months, the response values strongly increased at the other operating temperatures of 100, 125 and 175 °C, when compared to data presented in **Figure S3c**. For example, at 100 °C, the gas response value increased from ~5.5 to ~865. The increase at lower operating temperatures could be explained by temperature induced changes in the nanomaterial or contacts after the initial measurements, where the nano-sensor was heated up to 175 °C, which may act as a thermal treatment that strongly affects the structures of the nanosensor and reduces some defects on the surface of the material. These findings indicate that a short annealing step of the ZnO:Eu nanosensors strongly benefits the gas sensing properties towards room temperature sensing with a high gas response.

In addition, 10 months after the initial measurements the influence of relative humidity (RH%) on sensor performance was also investigated, since moisture is present in almost every practical application. Therefore, the ZnO:Eu₂₀ based nanosensor was tested to 100 ppm hydrogen at different RH% values measured at 10% and 50% and at different operating temperatures (see **Figure S5**). The maximum response of ~900 was achieved under conditions of 10% RH and an operating temperature of 150 °C. At an RH of 50% the maximum response decreased significantly to ~200 (at 125 °C). At all operating temperatures, the response value was higher at lower RH%, showing an increase by a factor of 3.5 – 8, which indicates that the humidity lowers the sensor's response values.

Please cite this paper as : C. Lupan, N. Wolff, J. Drewes, H. Krüger, A. Vahl, T. Pauporté, O. Lupan, B. Viana, L. Kienle, F. Faupel, R. Adelung, S. Hansen, Nanosensors Based on a Single ZnO:Eu Nanowire for Hydrogen Gas Sensing. ACS Appl. Mater. Interfaces, 14 (2022) 41196–41207. DOI: 10.1021/acsami.2c10975

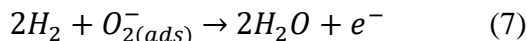
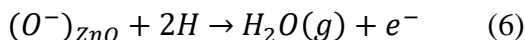
The sensing mechanism of the nanosensors based on ZnO:Eu nanowires can be explained by an adsorption-desorption process that takes place on the surface between the target gas and nanomaterial^{52,53}, producing a reversible modification of the nano-sensor parameters, for example electrical resistance^{38,54}.

At different operating temperatures, different oxygen species are adsorbed on the ZnO:Eu surface^{52,53}, so when we obtain a response at an operating temperature under 150 °C, interaction takes place between molecular oxygen O₂ and the target gas^{52–54}. At operating temperatures above 150 °C, interaction takes place between atomic oxygen species O[•] and O²⁻ and the target gas. Interactions between oxygen and the target gas can be summarized by the following reactions³⁸:



Since we observed a selectivity to 100 ppm hydrogen gas, the detection mechanism will be based on the interaction between hydrogen and oxygen species adsorbed on the surface of the ZnO:Eu nanowire and the Eu₂O₃ nanoparticles on its surface. After applying hydrogen, which is a reductive gas, the nano-sensor based on a *n*-type material will decrease its electrical resistance and increase its current, as shown in sensor measurements (see **Figure 6a, 7b**).

At room temperature, interactions that take place, can be summed up by the following reactions^{38,54}:



After the hydrogen gas is removed, electrical resistance return to its initial level after some time.

Mixing ZnO with surface deposited Eu results in electrical charge transfer between Zn²⁺ and Eu³⁺ with increasing Eu concentration, which changes the electronic properties of Zn, such as changing the electric field and increasing the electron density²³, observing a tendency of increase of initial electrical resistance at room temperatures for nanosensors with different Eu concentration, as shown in **Figure S6**. The enhanced hydrogen response of ZnO:Eu compared to ZnO may be due to

Please cite this paper as : C. Lupan, N. Wolff, J. Drewes, H. Krüger, A. Vahl, T. Pauporté, O. Lupan, B. Viana, L. Kienle, F. Faupel, R. Adelung, S. Hansen, Nanosensors Based on a Single ZnO:Eu Nanowire for Hydrogen Gas Sensing. ACS Appl. Mater. Interfaces, 14 (2022) 41196–41207. DOI: 10.1021/acsami.2c10975
this electrical charge transfer, which leads to a higher coverage of the surface with oxygen species due to a higher number of free electrons ²³.

3.6 DFT modeling: ZnO:Eu surface-H₂ gas molecule interaction

As described in the *Computational Methodology* section, we started with our earlier surface models ²⁷, considering the most stable termination of the ZnO (10 $\bar{1}$ 0) surface (shown in **Figure S7** and described in **Text S1**), based on the calculated surface energies from our earlier work ²⁷ and other works in the literature ^{55,56}. The slab comprised a total of 6 atomic layers, where the atomic coordinates of the bottom four layers were frozen at their bulk positions. We first investigated H₂ gas molecule interaction with ZnO (10 $\bar{1}$ 0) surface and found that the molecule interacts very weakly with no direct bond between surface and molecule. The hydrogen molecule exhibits physisorption with interaction energy of -21.3 kJ/mol. This is similar to our earlier work employing DFT-D2 approach ⁵⁷, where very weak interaction was found with interaction energy of -24.9 kJ/mol ²⁷. This small variation in interaction energy values is due to different level of dispersion correction functional used in the present work ³⁶.

Further, in order to model ZnO:Eu structures, we started from a 4x4 supercell of the ZnO (10 $\bar{1}$ 0) surface replacing the most exposed surface Zn atom with an Eu atom. Here, we note that, the Eu atom bonds to three surface oxygen atoms in the same top layer (bond lengths varying from 2.22 Å to 2.69 Å) and one oxygen atom in the second layer beneath (**Figure S8**). This structure was the most stable with having the lowest ground state energy ²⁷, compared to Eu doping on other surface sites in the top surface layer or sub-surface layers. Next, we investigated the interaction of an H₂ gas molecule with this single atom Eu in ZnO:Eu (10 $\bar{1}$ 0) surface, by placing the molecule in different initial orientations to the surface and exploring different surface adsorption sites. We note that the H₂ molecule shows weak interaction with the surface, with one of the hydrogen atoms forming a weak bond with the surface oxygen atom with a bond length of H-O = 2.31 Å (**Figure 9a**). As a result of the surface oxygen interacting with the H₂ molecule, the Zn-O bond length increases from 1.94 to 1.95 Å, as the oxygen atom moves upwards to bind the H₂ molecule, with a binding energy of -28.94 kJ/mol.

In order to investigate the presence of more Eu atoms on the surface, we further doped the ZnO:Eu surface with one more Eu atom by replacing another nearby exposed surface Zn atom to

Please cite this paper as : C. Lupan, N. Wolff, J. Drewes, H. Krüger, A. Vahl, T. Pauporté, O. Lupan, B. Viana, L. Kienle, F. Faupel, R. Adelung, S. Hansen, Nanosensors Based on a Single ZnO:Eu Nanowire for Hydrogen Gas Sensing. ACS Appl. Mater. Interfaces, 14 (2022) 41196–41207. DOI: 10.1021/acsami.2c10975

mimic the formation of a ZnO:Eu₂O₃ surface. Surface rearrangement takes place, where each substituted Eu atom bonds to four nearby oxygen atoms with bond lengths varying from 2.21 Å to 2.76 Å (**Figure S9**). In order to further investigate the surface-H₂ interaction, we placed an H₂ molecule close to the Eu atoms in different orientations and observed that the H₂ molecule binds comparatively stronger with this surface. One of the hydrogen atoms interacts with two surface oxygen atoms, at distances of 2.39 and 2.89 Å (**Figure 9b**). The surface Eu atom also moves upwards to bind the H₂ molecule at a distance of 2.72 Å. As a result of this Eu-H₂ molecule interaction, the surface Eu-O bonds elongate and the bond length of the Eu atom with the sublayer oxygen atom increases from 2.21 to 2.22 Å, as oxygen atoms move to bind with the H₂ molecule. The presence of two Eu atoms in the ZnO (10 $\bar{1}$ 0) surface results in comparatively better interaction of the H₂ molecule with the surface due to the presence of more valence electrons, thereby increasing the activity of the surface with interaction energy of -30 kJ/mol. The surface-H₂ molecule interaction is reflected in our charge density difference plot as well, where we note significant charge redistribution, as the surface oxygen atom loses electrons (Bader charge -1.20 e⁻), while the Eu atom gains electrons (Bader charge 1.36 e⁻), as denoted in **Figure 10a** by yellow and blue colored iso-surfaces, respectively. The H₂ interaction is also reflected in terms of changes in the Fermi energy, as E_F shifts to -1.59 eV from -1.61 eV.

In order to investigate the effect of humidity, we next investigated the interaction of a water molecule with the Eu₂:ZnO surface with the pre-adsorbed H₂ molecule, where we found that as soon as the water molecule comes into contact with the surface Eu atoms, it spontaneously dissociates into H and OH species. The H⁺ ion bonds with a surface O atom, that is connected to an Eu atom, while the OH species binds the two Eu atoms, as shown in **Figure 10b**. As a result, the H₂ molecule now interacts comparatively weaker with the surface, increasing the H-O (hydrogen atom to surface oxygen atom) distance to 2.44 Å and the H-Eu distance to 2.81 Å. As such, we consider that in the presence of more water molecules, surface oxygen and Eu sites will become covered by water, thereby decreasing the sensitivity of the surface towards H₂ gas molecules.

4 CONCLUSIONS

Please cite this paper as : C. Lupan, N. Wolff, J. Drewes, H. Krüger, A. Vahl, T. Pauporté, O. Lupan, B. Viana, L. Kienle, F. Faupel, R. Adelung, S. Hansen, Nanosensors Based on a Single ZnO:Eu Nanowire for Hydrogen Gas Sensing. ACS Appl. Mater. Interfaces, 14 (2022) 41196–41207. DOI: 10.1021/acsami.2c10975

In this study, the effects of Eu concentration in the electrolyte bath (ranging from 0 μM to 20 μM) on the morphology, structure, chemical, optical, electrical as well as on the gas sensing characteristics of ZnO:Eu nanowires with good crystallinity is described. The addition of Eu (3–20 μM Eu ions in the electrolyte) and simultaneous functionalization of the surface with europium oxide agglomerates resulted in high selectivity and excellent sensitivity to hydrogen gas, leading to a maximum gas response of ~ 7860 at 100 ppm H_2 and an operating temperature of 150 $^\circ\text{C}$. DFT simulations also confirm that Eu mixing concentration increases the activity of the ZnO surface and the Eu-mixed material shows better sensitivity towards the H_2 gas. For the sample containing 5 μM Eu, both hydrogen and UV responses were detected even at room temperature, which is essential to detect the flame generated by a hydrogen-oxygen mixture. The combustion flames emit UV radiation and the application requires the need to heat the sensor to be eliminated. We demonstrated a possibility for a new type of dual-mode nano-sensor to detect UV/ H_2 gas simultaneously for selective detection of H_2 during UV irradiation.

To test the nano-sensor's ability to reliably detect hydrogen leaks in different environments, the effect of humidity on the sensing properties was investigated. A decrease in response to hydrogen by a factor of 3.5 to 8 was observed with 50% RH at different operating temperatures, but this sensor remained selective and sensitive. DFT simulations indicate that the H_2O molecule interacts with Eu sites on the ZnO surface, thereby lowering the interaction and sensitivity towards H_2 gas molecules.

Nanosensors based on ZnO:Eu nanowires have shown an increase in electrical conductivity upon exposure to H_2 , demonstrating the *n*-type conductivity of the nanowires, which involves the formation of oxygen species that interact with the ZnO:Eu nanosensor surface.

Please cite this paper as : C. Lupan, N. Wolff, J. Drewes, H. Krüger, A. Vahl, T. Pauporté, O. Lupan, B. Viana, L. Kienle, F. Faupel, R. Adelung, S. Hansen, Nanosensors Based on a Single ZnO:Eu Nanowire for Hydrogen Gas Sensing. ACS Appl. Mater. Interfaces, 14 (2022) 41196–41207. DOI: 10.1021/acsami.2c10975

The results obtained for a sensor based on a single ZnO:Eu nanowire can be used to further enhance the growth parameters, such as doping or mixing content, to enhance the response to hydrogen gas and UV radiation down to room temperature, to develop dual-mode nano-sensors and to integrate the material into devices for personal, industrial, safety and environmental use.

■ ASSOCIATED CONTENT

Supporting Information: TEM images of ZnO:Eu nanowire showing its morphology at a large scale and higher magnification of one nanowire functionalized with a porous network coating of Eu_2O_3 . Compositional images measured by elemental EDX mapping at the microstructural level of ZnO:Eu deposition and EDX spectra. Summary of the UV nanosensors based on ZnO:Eu5 and to 100 ppm of hydrogen gas in air at different operating temperatures and RH%. Response to UV light and 100 ppm hydrogen for ZnO:Eu3 nanosensor at 100 °C. Gas response for 100 ppm of different gases at various operating temperature for ZnO:Eu 6, 10, and 20. Comparison of the gas response at different operating temperature for ZnO:Eu20 nanosensor. Gas response for ZnO:Eu20 nanosensor at two different relative humidities (RH%). Comparison of initial electrical resistance for different Eu concentration nanosensors at room temperature. DFT modeling of ZnO and ZnO:Eu structure. Relaxed structure of one and two Eu atoms doped in ZnO (10 $\bar{1}$ 0) surface. The Supporting Information is available free of charge on the ACS Publications website at <http://pubs.acs.org>

■ AUTHOR INFORMATION

Corresponding Authors

*E-mails: ollu@tf.uni-kiel.de, oleg.lupan@mib.utm.md (O.L.); akmishra@ddn.upes.ac.in (A.K.M); cristian.lupan@mib.utm.md (C.L.); alva@tf.uni-kiel.de (A.V.); sn@tf.uni-kiel.de (S.N.).

Please cite this paper as : C. Lupan, N. Wolff, J. Drewes, H. Krüger, A. Vahl, T. Pauporté, O. Lupan, B. Viana, L. Kienle, F. Faupel, R. Adelung, S. Hansen, Nanosensors Based on a Single ZnO:Eu Nanowire for Hydrogen Gas Sensing. ACS Appl. Mater. Interfaces, 14 (2022) 41196–41207. DOI: 10.1021/acsami.2c10975

Notes

The authors declare no competing interest.

Author Contributions

The manuscript was written through contributions of all authors. All authors have given approval to the final version of the manuscript. C.L., Th.P. and O.L. carried out laboratory research synthesized the ZnO:Eu nanomaterial. C.L., N.W., J.D. wrote draft of manuscript. N.W. and L.K. performed all TEM, EDS experiments and data analysis. J.D., and A.V. realized all XPS experiments and data analysis. C.L., O.L. and R.A. adapted technological approach for material integration/fabrication of the sensors for gas detection and SEM-EDX FIB-SEM laboratory research. C.L. carried out laboratory research and the measurement of sensing properties of sensors based on such structures and analyzed all data. C.L., Th.P., B.V. and O.L. realized all optical experiments and data analysis. S.H., H.K., O.L. and R.A. study conception for battery safety application. C.L., N.W., Th.P., R.A., and A.V. analyzed the results, including experimental data and revised draft. C.L., N.W., A.V., H.K., and R.A. drafting the article. A.K.M. carried out DDTT calculations and together with N.H.d.L. drafted the computational part for the manuscript. C.L., S.H., Th.P. and R.A. study conception and design, final approval of the version to be published. All authors reviewed the manuscript.

Funding Sources

Project “SuSiBaBy” - SulfurSilicon Batteries by the EUSH and EFRE in SH (LPW-E/3.1.1/1801). Federal Ministry of Education and Research by funding the former “PorSSi” project (03XP0126 A & B).

Please cite this paper as : C. Lupan, N. Wolff, J. Drewes, H. Krüger, A. Vahl, T. Pauporté, O. Lupan, B. Viana, L. Kienle, F. Faupel, R. Adelung, S. Hansen, Nanosensors Based on a Single ZnO:Eu Nanowire for Hydrogen Gas Sensing. ACS Appl. Mater. Interfaces, 14 (2022) 41196–41207. DOI: 10.1021/acsami.2c10975 German Research Foundation (DFG- Deutsche Forschungsgemeinschaft) under the schemes SFB1261, SFB 1461 & AD 183/16-1. Funded by the Deutsche Forschungsgemeinschaft (DFG, German Research Foundation) – Project-ID 434434223 – SFB 1461. The ANCD-NARD Grant No. 20.80009.5007.09 at the Technical University of Moldova.

(DFG - Deutsche Forschungsgemeinschaft) under the schemes FOR 2093 and AD 183/18-1.

ACKNOWLEDGMENTS

C. Lupan gratefully acknowledges Kiel University, Functional Nanomaterials, Germany and PSL Université, Chimie-ParisTech IRCP, Paris, France for internship positions in 2018-2019 and TUM, Chisinau, Republic of Moldova, for constant support. C. Lupan would like to express special appreciation and thanks to Professor Trofim Viorel (TUM) as MSc Thesis supervisor, for the encouragement, fruitful discussions on this work, patient guidance, and advice he has provided throughout time. Funded by the Deutsche Forschungsgemeinschaft (DFG, German Research Foundation) – Project-ID 434434223 – SFB 1461 and SFB 1261. This work was partially supported by the Technical University of Moldova and through the ANCD-NARD Grant No. 20.80009.5007.09 at TUM. This investigation was partially supported by the German Research Foundation (DFG - Deutsche Forschungsgemeinschaft) under the schemes FOR 2093 and AD 183/18-1. We acknowledge funding within the project “SuSiBaBy” - SulfurSilicon Batteries by the EUSH and EFRE in SH (LPW-E/3.1.1/1801). We are especially grateful to the Federal Ministry of Education and Research by funding the former “PorSSi” project (03XP0126 A & B). Katrin Brandenburg is acknowledged for her help in the final proof-reading of the manuscript.

This work used the ARCHER2 UK National Supercomputing Service (<https://www.archer2.ac.uk>). AKM acknowledges SEED grant (2021) from UPES, Dehradun.

Please cite this paper as : C. Lupan, N. Wolff, J. Drewes, H. Krüger, A. Vahl, T. Pauporté, O. Lupan, B. Viana, L. Kienle, F. Faupel, R. Adelung, S. Hansen, Nanosensors Based on a Single ZnO:Eu Nanowire for Hydrogen Gas Sensing. *ACS Appl. Mater. Interfaces*, 14 (2022) 41196–41207. DOI: 10.1021/acsami.2c10975

References

- (1) Saeedmanesh, A.; Mac Kinnon, M. A.; Brouwer, J. Hydrogen Is Essential for Sustainability. *Curr. Opin. Electrochem.* **2018**, 12, 166–181.
- (2) Arshad, F.; Haq, T. ul; Hussain, I.; Sher, F. Recent Advances in Electrocatalysts toward Alcohol-Assisted, Energy-Saving Hydrogen Production. *ACS Appl. Energy Mater.* **2021**, 4 (9), 8685–8701.
- (3) Ohsaki, T.; Kishi, T.; Kuboki, T.; Takami, N.; Shimura, N.; Sato, Y.; Sekino, M.; Satoh, A. Overcharge Reaction of Lithium-Ion Batteries. *J. Power Sources* **2005**, 146 (1–2), 97–100.
- (4) Essl, C.; Golubkov, A. W.; Fuchs, A. Comparing Different Thermal Runaway Triggers for Two Automotive Lithium-Ion Battery Cell Types. *J. Electrochem. Soc.* **2020**, 167 (13), 130542.
- (5) *Guide for the Ventilation and Thermal Management of Batteries for Stationary Applications*; IEEE, 2018.
- (6) Chen, Y.; Kang, Y.; Zhao, Y.; Wang, L.; Liu, J.; Li, Y.; Liang, Z.; He, X.; Li, X.; Tavajohi, N.; Li, B. A Review of Lithium-Ion Battery Safety Concerns: The Issues, Strategies, and Testing Standards. *J. Energy Chem.* **2021**, 59, 83–99.
- (7) Sundén, B. Battery Technologies. *Hydrog. Batter. Fuel Cells* **2019**, 57–79.
- (8) Hosseini, S. E.; Wahid, M. A. Hydrogen from Solar Energy, a Clean Energy Carrier from a Sustainable Source of Energy. *Int. J. Energy Res.* **2020**, 44 (6), 4110–4131.
- (9) Essl, C.; Golubkov, A. W.; Gasser, E.; Nachtnebel, M.; Zankel, A.; Ewert, E.; Fuchs, A. Comprehensive Hazard Analysis of Failing Automotive Lithium-ion Batteries in Overtemperature Experiments. *Batteries* **2020**, 6 (2), 30.
- (10) Golubkov, A. W.; Scheikl, S.; Planteu, R.; Voitic, G.; Wiltsche, H.; Stangl, C.; Fauler, G.; Thaler, A.; Hacker, V. Thermal Runaway of Commercial 18650 Li-Ion Batteries with LFP and NCA Cathodes - Impact of State of Charge and Overcharge. *RSC Adv.* **2015**, 5 (70), 57171–57186.

- Please cite this paper as** : C. Lupan, N. Wolff, J. Drewes, H. Krüger, A. Vahl, T. Pauporté, O. Lupan, B. Viana, L. Kienle, F. Faupel, R. Adelung, S. Hansen, Nanosensors Based on a Single ZnO:Eu Nanowire for Hydrogen Gas Sensing. *ACS Appl. Mater. Interfaces*, 14 (2022) 41196–41207. DOI: 10.1021/acsami.2c10975
- (11) International Code Council. *2018 International Fire Code*; International Code Council, 2017.
 - (12) Carcassi, M. N.; Fineschi, F. Deflagrations of H₂-Air and CH₄-Air Lean Mixtures in a Vented Multi-Compartment Environment. *Energy* **2005**, 30 (8 SPEC. ISS.), 1439–1451.
 - (13) Lupan, O.; Cretu, V.; Postica, V.; Ahmadi, M.; Cuenya, B. R.; Chow, L.; Tiginyanu, I.; Viana, B.; Pauporté, T.; Adelung, R. Silver-Doped Zinc Oxide Single Nanowire Multifunctional Nanosensor with a Significant Enhancement in Response. *Sensors Actuators, B Chem.* **2016**, 223, 893–903.
 - (14) Gorup, L. F.; Amorin, L. H.; Camargo, E. R.; Sequinel, T.; Cincotto, F. H.; Biasotto, G.; Ramesar, N.; La Porta, F. de A. Methods for Design and Fabrication of Nanosensors: The Case of ZnO-Based Nanosensor. *Nanosensors for Smart Cities* **2020**, 9–30.
 - (15) Hastir, A.; Kohli, N.; Singh, R. C. Comparative Study on Gas Sensing Properties of Rare Earth (Tb , Dy and Er) Doped ZnO Sensor. *J. Phys. Chem. Solids* **2017**, 105 (January), 23–34.
 - (16) Lupan, O.; Postica, V.; Pauporté, T.; Viana, B.; Terasa, M. I.; Adelung, R. Room Temperature Gas Nanosensors Based on Individual and Multiple Networked Au-Modified ZnO Nanowires. *Sensors Actuators, B Chem.* **2019**, 299 (July), 126977.
 - (17) Lupan, O.; Postica, V.; Wolff, N.; Su, J.; Labat, F.; Ciofini, I.; Cavers, H.; Adelung, R.; Polonskyi, O.; Faupel, F.; Kienle, L.; Viana, B.; Pauporté, T. Lowerature Solution Synthesis of Au-Modified ZnO Nanowires for Highly Efficient Hydrogen Nanosensors. *ACS Appl. Mater. Interfaces* **2019**, 11 (35), 32115–32126.
 - (18) Postica, V.; Vahl, A.; Santos-Carballal, D.; Dankwort, T.; Kienle, L.; Hoppe, M.; Cadi-Essadek, A.; De Leeuw, N. H.; Terasa, M. I.; Adelung, R.; Faupel, F.; Lupan, O. Tuning ZnO Sensors Reactivity toward Volatile Organic Compounds via Ag Doping and Nanoparticle Functionalization. *ACS Appl. Mater. Interfaces* **2019**, 11 (34), 31452–31466.
 - (19) Han, D.; Yang, J.; Gu, F.; Wang, Z. Effects of Rare Earth Element Doping on the Ethanol Gas-Sensing Performance of Three-Dimensionally Ordered Macroporous In₂O₃. *RSC Adv.* **2016**, 6 (51), 45085–45092.

- Please cite this paper as** : C. Lupan, N. Wolff, J. Drewes, H. Krüger, A. Vahl, T. Pauporté, O. Lupan, B. Viana, L. Kienle, F. Faupel, R. Adelung, S. Hansen, Nanosensors Based on a Single ZnO:Eu Nanowire for Hydrogen Gas Sensing. *ACS Appl. Mater. Interfaces*, 14 (2022) 41196–41207. DOI: 10.1021/acscami.2c10975
- (20) Dash, D.; Panda, N. R.; Sahu, D. Photoluminescence and Photocatalytic Properties of Europium Doped ZnO Nanoparticles. *Appl. Surf. Sci.* **2019**, 494, 666–674.
- (21) Pauporté, T.; Pellé, F.; Viana, B.; Aschehoug, P. Luminescence of Nanostructured Eu³⁺/ZnO Mixed Films Prepared by Electrodeposition. *J. Phys. Chem. C* **2007**, 111 (42), 15427–15432.
- (22) Zhao, S.; Shen, Y.; Li, A.; Chen, Y.; Gao, S.; Liu, W.; Wei, D. Effects of Rare Earth Elements Doping on Gas Sensing Properties of ZnO Nanowires. *Ceram. Int.* **2021**, 47 (17), 24218–24226.
- (23) Lupan, C.; Khaledialidusti, R.; Mishra, A. K.; Postica, V.; Terasa, M. I.; Magariu, N.; Pauporté, T.; Viana, B.; Drewes, J.; Vahl, A.; Faupel, F.; Adelung, R. Pd-Functionalized ZnO:Eu Columnar Films for Room-Temperature Hydrogen Gas Sensing: A Combined Experimental and Computational Approach. *ACS Appl. Mater. Interfaces* **2020**, 12 (22), 24951–24964.
- (24) Lupan, O.; Pauporté, T.; Viana, B.; Aschehoug, P.; Ahmadi, M.; Cuenya, B. R.; Rudzevich, Y.; Lin, Y.; Chow, L. Eu-Doped ZnO Nanowire Arrays Grown by Electrodeposition. *Appl. Surf. Sci.* **2013**, 282, 782–788.
- (25) Moulder, J. F.; Stickle, W. F.; Sobol, P. E.; Bomben, K. D. Handbook of Photoelectron Spectroscopy. *Phys. Electron. Inc., Eden Prairie, Minnesota* **1992**.
- (26) Kohlmann, N.; Hansen, L.; Lupan, C.; Schu, U.; Reimers, A.; Schu, F.; Adelung, R.; Kersten, H.; Kienle, L. Fabrication of ZnO Nanobrushes by H₂ – C₂H₂ Plasma Etching for H₂ Sensing Applications. **2021**, 13 (51), 61758–61769.
- (27) Lupan, O.; Magariu, N.; Khaledialidusti, R.; Mishra, A. K.; Hansen, S.; Krüger, H.; Postica, V.; Heinrich, H.; Viana, B.; Ono, L. K.; Cuenya, B. R.; Chow, L.; Adelung, R.; Pauporté, T. Comparison of Thermal Annealing versus Hydrothermal Treatment Effects on the Detection Performances of ZnO Nanowires. *ACS Appl. Mater. Interfaces* **2021**, 13 (8), 10537–10552.
- (28) Lupan, O.; Chai, G.; Chow, L. Fabrication of ZnO Nanorod-Based Hydrogen Gas Nanosensor. *Microelectronics J.* **2007**, 38 (12), 1211–1216.

- Please cite this paper as** : C. Lupan, N. Wolff, J. Drewes, H. Krüger, A. Vahl, T. Pauporté, O. Lupan, B. Viana, L. Kienle, F. Faupel, R. Adelung, S. Hansen, Nanosensors Based on a Single ZnO:Eu Nanowire for Hydrogen Gas Sensing. *ACS Appl. Mater. Interfaces*, 14 (2022) 41196–41207. DOI: 10.1021/acsami.2c10975
- (29) Perdew, J. P.; Burke, K.; Ernzerhof, M. Generalized Gradient Approximation Made Simple. *Phys. Rev. Lett.* **1996**, 77 (18), 3865–3868.
- (30) Blöchl, P. E. Projector Augmented-Wave Method. *Phys. Rev. B* **1994**, 50 (24), 17953–17979.
- (31) Kresse, G.; Joubert, D. From Ultrasoft Pseudopotentials to the Projector Augmented-Wave Method. *Phys. Rev. B* **1999**, 59 (3), 11–19.
- (32) Kresse, G.; Furthmüller, J. Efficiency of Ab-Initio Total Energy Calculations for Metals and Semiconductors Using a Plane-Wave Basis Set. *Comput. Mater. Sci.* **1996**, 6 (1), 15–50.
- (33) Postica, V.; Gröttrup, J.; Adelung, R.; Lupan, O.; Mishra, A. K.; de Leeuw, N. H.; Ababii, N.; Carreira, J. F. C.; Rodrigues, J.; Sedrine, N. Ben; Correia, M. R.; Monteiro, T.; Sontea, V.; Mishra, Y. K. Multifunctional Materials: A Case Study of the Effects of Metal Doping on ZnO Tetrapods with Bismuth and Tin Oxides. *Adv. Funct. Mater.* **2017**, 27 (6), 1604676.
- (34) Lupan, O.; Postica, V.; Gröttrup, J.; Mishra, A. K.; De Leeuw, N. H.; Carreira, J. F. C.; Rodrigues, J.; Ben Sedrine, N.; Correia, M. R.; Monteiro, T.; Cretu, V.; Tiginyanu, I.; Smazna, D.; Mishra, Y. K.; Adelung, R. Hybridization of Zinc Oxide Tetrapods for Selective Gas Sensing Applications. *ACS Appl. Mater. Interfaces* **2017**, 9 (4), 4084–4099.
- (35) Pack, J. D.; Monkhorst, H. J. “special Points for Brillouin-Zone Integrations”-a Reply. *Phys. Rev. B* **1977**, 16 (4), 1748–1749.
- (36) Grimme, S.; Antony, J.; Ehrlich, S.; Krieg, H. A Consistent and Accurate Ab Initio Parametrization of Density Functional Dispersion Correction (DFT-D) for the 94 Elements H-Pu. *J. Chem. Phys.* **2010**, 132 (15), 154104.
- (37) Henkelman, G.; Arnaldsson, A.; Jónsson, H. A Fast and Robust Algorithm for Bader Decomposition of Charge Density. *Comput. Mater. Sci.* **2006**, 36 (3), 354–360.
- (38) Lupan, O.; Chai, G.; Chow, L. Novel Hydrogen Gas Sensor Based on Single ZnO Nanorod. *Microelectron. Eng.* **2008**, 85 (11), 2220–2225.
- (39) Lupan, O.; Ursaki, V. V.; Chai, G.; Chow, L.; Emelchenko, G. A.; Tiginyanu, I. M.; Gruzintsev, A. N.; Redkin, A. N. Selective Hydrogen Gas Nanosensor Using Individual ZnO

- Please cite this paper as** : C. Lupan, N. Wolff, J. Drewes, H. Krüger, A. Vahl, T. Pauporté, O. Lupan, B. Viana, L. Kienle, F. Faupel, R. Adelung, S. Hansen, Nanosensors Based on a Single ZnO:Eu Nanowire for Hydrogen Gas Sensing. *ACS Appl. Mater. Interfaces*, 14 (2022) 41196–41207. DOI: 10.1021/acsami.2c10975
Nanowire with Fast Response at Room Temperature. *Sensors Actuators, B Chem.* **2010**, 144 (1), 56–66.
- (40) Hocking, W. H.; Matthew, J. A. D. Electron Spectroscopy of Europium. *J. Phys. Condens. Matter* **1990**, 2 (15), 3643–3658.
- (41) Tizei, L. H. G.; Nakanishi, R.; Kitaura, R.; Shinohara, H.; Suenaga, K. Core-Level Spectroscopy to Probe the Oxidation State of Single Europium Atoms. *Phys. Rev. Lett.* **2015**, 114 (19), 197602.
- (42) Mundy, J. A.; Hodash, D.; Melville, A.; Held, R.; Mairoser, T.; Muller, D. A.; Kourkoutis, L. F.; Schmehl, A.; Schlom, D. G. Hetero-Epitaxial EuO Interfaces Studied by Analytic Electron Microscopy. *Appl. Phys. Lett.* **2014**, 104 (9), 091601.
- (43) Mairoser, T.; Mundy, J. A.; Melville, A.; Hodash, D.; Cueva, P.; Held, R.; Glavic, A.; Schubert, J.; Muller, D. A.; Schlom, D. G.; Schmehl, A. High-Quality EuO Thin Films the Easy Way via Topotactic Transformation. *Nat. Commun.* **2015**, 6, 1–7.
- (44) Postica, V.; Vahl, A.; Strobel, J.; Santos-Carballal, D.; Lupan, O.; Cadi-Essadek, A.; De Leeuw, N. H.; Schütt, F.; Polonskyi, O.; Strunskus, T.; Baum, M.; Kienle, L.; Adelung, R.; Faupel, F. Tuning Doping and Surface Functionalization of Columnar Oxide Films for Volatile Organic Compound Sensing: Experiments and Theory. *J. Mater. Chem. A* **2018**, 6 (46), 23669–23682.
- (45) Lupan, O.; Emelchenko, G. A.; Ursaki, V. V.; Chai, G.; Redkin, A. N.; Gruzintsev, A. N.; Tiginyanu, I. M.; Chow, L.; Ono, L. K.; Roldan Cuenya, B.; Heinrich, H.; Yakimov, E. E. Synthesis and Characterization of ZnO Nanowires for Nanosensor Applications. *Mater. Res. Bull.* **2010**, 45 (8), 1026–1032.
- (46) Rumble, J. R.; Bickham, D. M.; Powell, C. J. The NIST X-ray Photoelectron Spectroscopy Database. *Surf. Interface Anal.* **1992**, 19 (1–12), 241–246.
- (47) Lupan, O.; Chai, G.; Chow, L.; Emelchenko, G. A.; Heinrich, H.; Ursaki, V. V.; Gruzintsev, A. N.; Tiginyanu, I. M.; Redkin, A. N. Ultraviolet Photoconductive Sensor Based on Single ZnO Nanowire. *Phys. Status Solidi Appl. Mater. Sci.* **2010**, 207 (7), 1735–1740.

Please cite this paper as : C. Lupan, N. Wolff, J. Drewes, H. Krüger, A. Vahl, T. Pauporté, O. Lupan, B. Viana, L. Kienle, F. Faupel, R. Adelung, S. Hansen, Nanosensors Based on a Single ZnO:Eu Nanowire for Hydrogen Gas Sensing. *ACS Appl. Mater. Interfaces*, 14 (2022) 41196–41207. DOI: 10.1021/acsami.2c10975

- (48) Rashid, T. R.; Phan, D. T.; Chung, G. S. A Flexible Hydrogen Sensor Based on Pd Nanoparticles Decorated ZnO Nanorods Grown on Polyimide Tape. *Sensors Actuators, B Chem.* **2013**, 185, 777–784.
- (49) Khan, R.; Ra, H. W.; Kim, J. T.; Jang, W. S.; Sharma, D.; Im, Y. H. Nanojunction Effects in Multiple ZnO Nanowire Gas Sensor. *Sensors Actuators, B Chem.* **2010**, 150 (1), 389–393.
- (50) Zhou, J.; Gu, Y.; Hu, Y.; Mai, W.; Yeh, P. H.; Bao, G.; Sood, A. K.; Polla, D. L.; Wang, Z. L. Gigantic Enhancement in Response and Reset Time of ZnO UV Nanosensor by Utilizing Schottky Contact and Surface Functionalization. *Appl. Phys. Lett.* **2009**, 94 (19), 191103.
- (51) Sihar, N.; Tiong, T. Y.; Dee, C. F.; Ooi, P. C.; Hamzah, A. A.; Mohamed, M. A.; Majlis, B. Y. Ultraviolet Light-Assisted Copper Oxide Nanowires Hydrogen Gas Sensor. *Nanoscale Res. Lett.* **2018**, 13, 4–9.
- (52) Yamazoe, N.; Fuchigami, J.; Kishikawa, M.; Seiyama, T. Interactions of Tin Oxide Surface with O₂, H₂O AND H₂. *Surf. Sci.* **1979**, 86 (C), 335–344.
- (53) Lenaerts, S.; Roggen, J.; Maes, G. FT-IR Characterization of Tin Dioxide Gas Sensor Materials under Working Conditions. *Spectrochim. Acta Part A Mol. Biomol. Spectrosc.* **1995**, 51 (5), 883–894.
- (54) Chang, S. C. Oxygen Chemisorption on Tin Oxide: Correlation Between Electrical Conductivity and Epr Measurements. *J. Vac. Sci. Technol.* **1979**, 17 (1), 366–369.
- (55) Cooke, D. J.; Marmier, A.; Parker, S. C. Surface Structure of (1010) and (1120) Surfaces of ZnO with Density Functional Theory and Atomistic Simulation. *J. Phys. Chem. B* **2006**, 110 (15), 7985–7991.
- (56) Wander, A.; Harrison, N. M. Ab-Initio Study of ZnO(1120). *Surf. Sci.* **2000**, 468 (1–3), 851–855.
- (57) Grimme, S. Semiempirical GGA-Type Density Functional Constructed with a Long-Range Dispersion Correction. *Comput. Chem.* **2006**, 27, 1787–1799.

Please cite this paper as : C. Lupan, N. Wolff, J. Drewes, H. Krüger, A. Vahl, T. Pauporté, O. Lupan, B. Viana, L. Kienle, F. Faupel, R. Adelung, S. Hansen, Nanosensors Based on a Single ZnO:Eu Nanowire for Hydrogen Gas Sensing. ACS Appl. Mater. Interfaces, 14 (2022) 41196–41207. DOI: 10.1021/acsami.2c10975

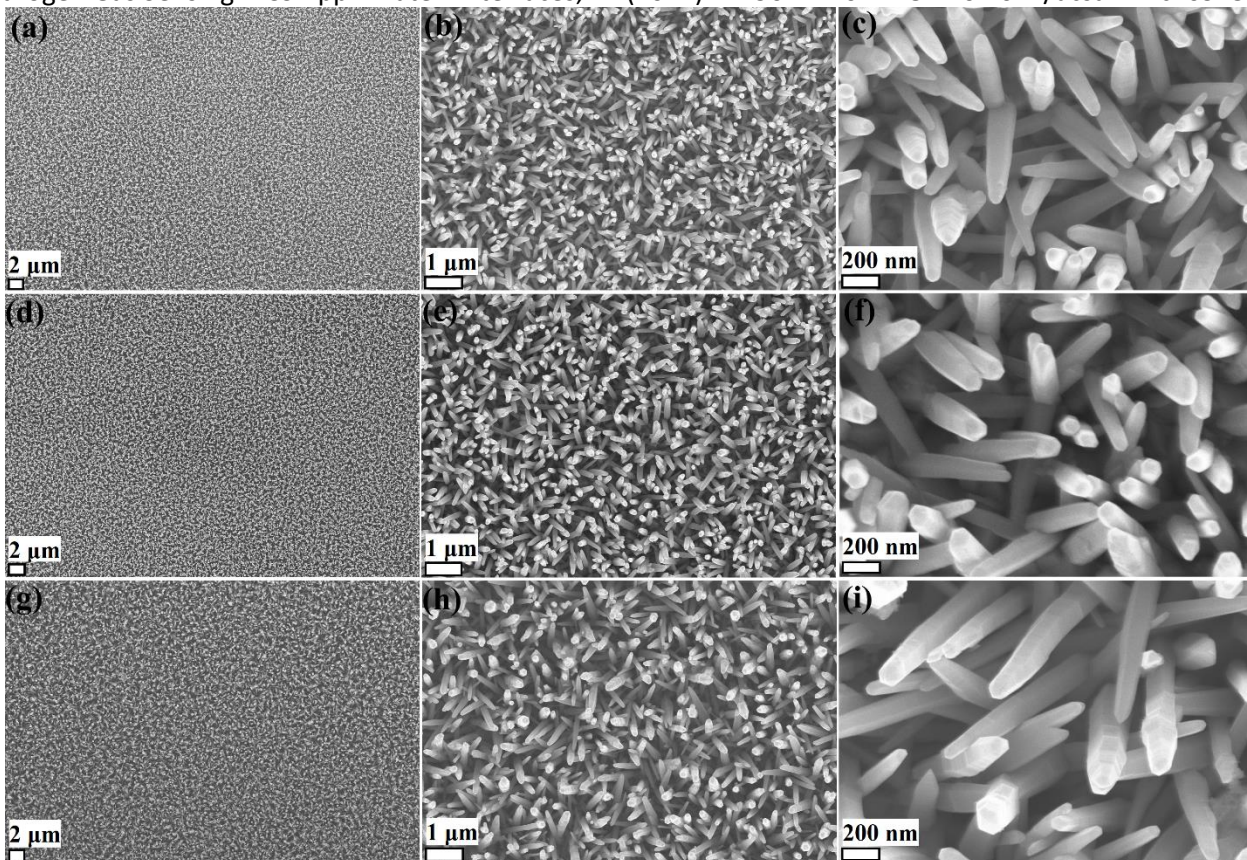


Figure 1. SEM images of ZnO:Eu nanowire arrays grown in electrolyte solution with EuCl_3 concentration of: (a-c) – 3 μM ; (d-f) – 5 μM ; (g-i) – 10 μM . The magnification increases from left to right.

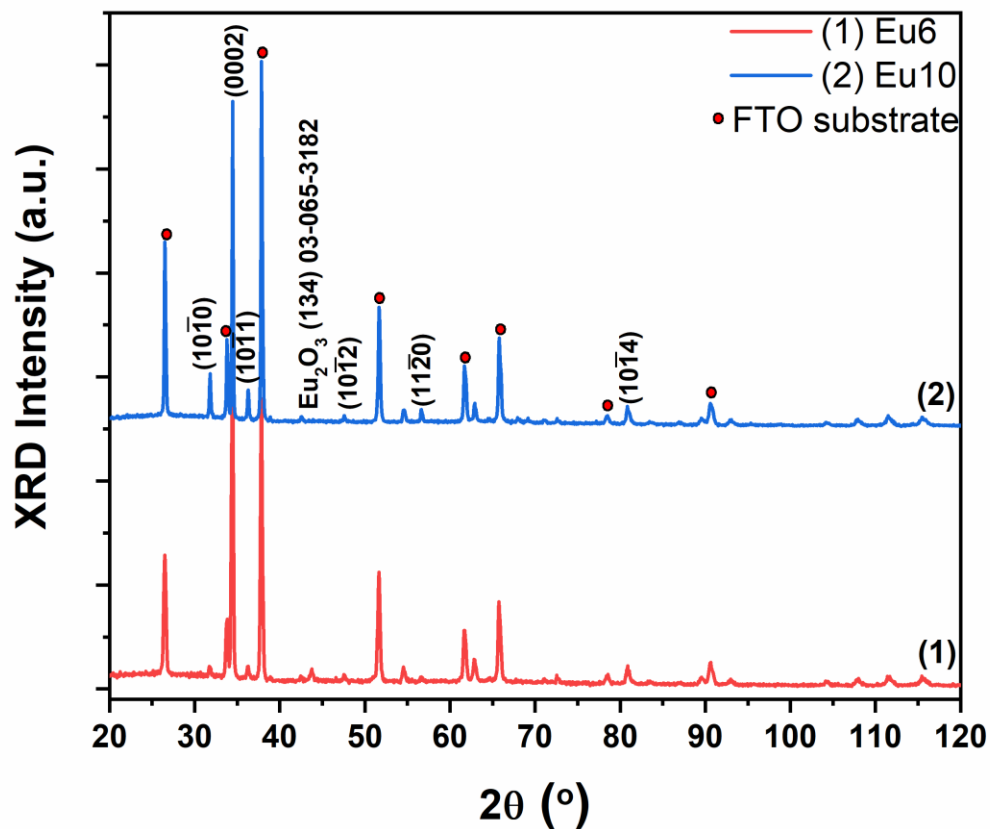


Figure 2. XRD pattern of ZnO:Eu nanowires grown by electrochemical deposition with different Eu concentrations: 6 and 10 μM EuCl_3 content in the electrolyte (samples: ZnO:Eu6 and ZnO:Eu10). Peaks from the used FTO substrate ($\text{SnO}_2\text{:F}$) are indicated by red circles.

Please cite this paper as : C. Lupan, N. Wolff, J. Drewes, H. Krüger, A. Vahl, T. Pauporté, O. Lupan, B. Viana, L. Kienle, F. Faupel, R. Adelung, S. Hansen, Nanosensors Based on a Single ZnO:Eu Nanowire for Hydrogen Gas Sensing. ACS Appl. Mater. Interfaces, 14 (2022) 41196–41207. DOI: 10.1021/acsami.2c10975

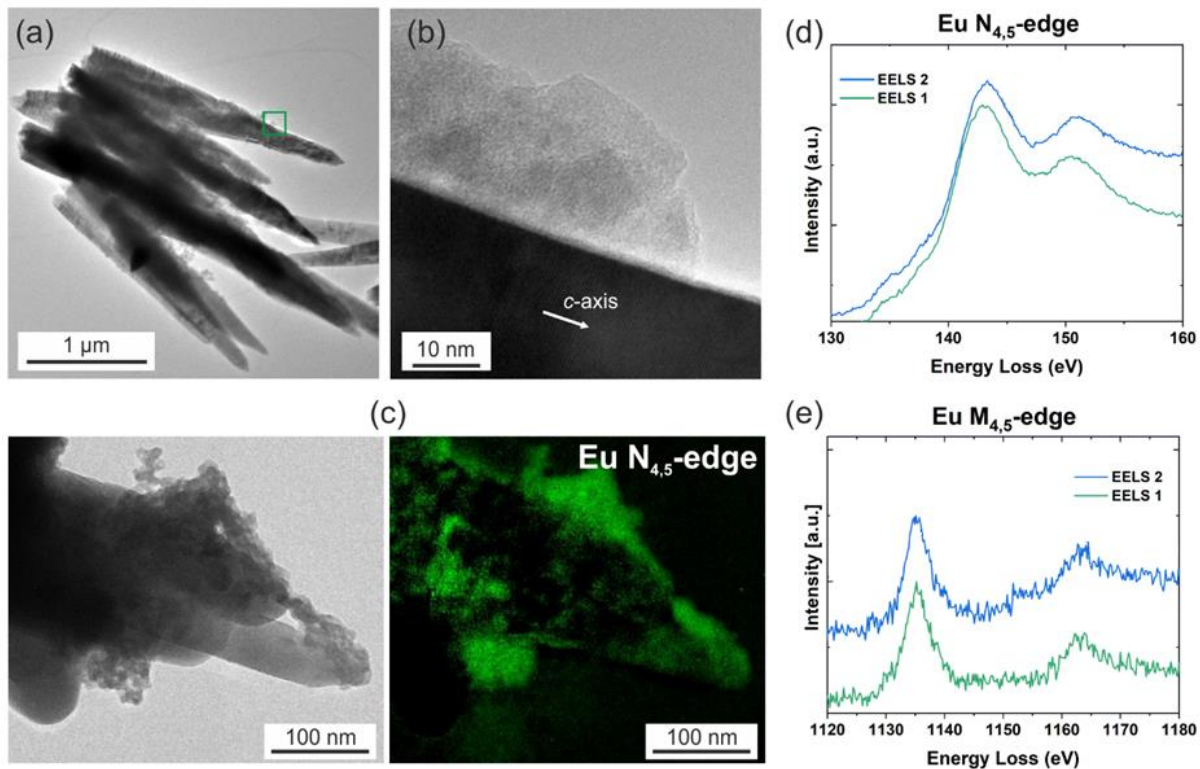


Figure 3. (a) TEM image of needle-shaped ZnO:Eu nanowires decorated with amorphous Eu-oxide species. (b) High-magnification micrograph showing the amorphous network covering the surface of the single crystalline ZnO nanowire. (c) Zero energy-loss filtered and EFTEM image recorded using the Eu N_{4,5}-edge. Electron energy-loss spectra recorded on Eu-networks are shown in (d) N_{4,5} and (e) M_{4,5}-edges, data of Eu³⁺.

Please cite this paper as : C. Lupan, N. Wolff, J. Drewes, H. Krüger, A. Vahl, T. Pauporté, O. Lupan, B. Viana, L. Kienle, F. Faupel, R. Adelung, S. Hansen, Nanosensors Based on a Single ZnO:Eu Nanowire for Hydrogen Gas Sensing. ACS Appl. Mater. Interfaces, 14 (2022) 41196–41207. DOI: 10.1021/acsami.2c10975

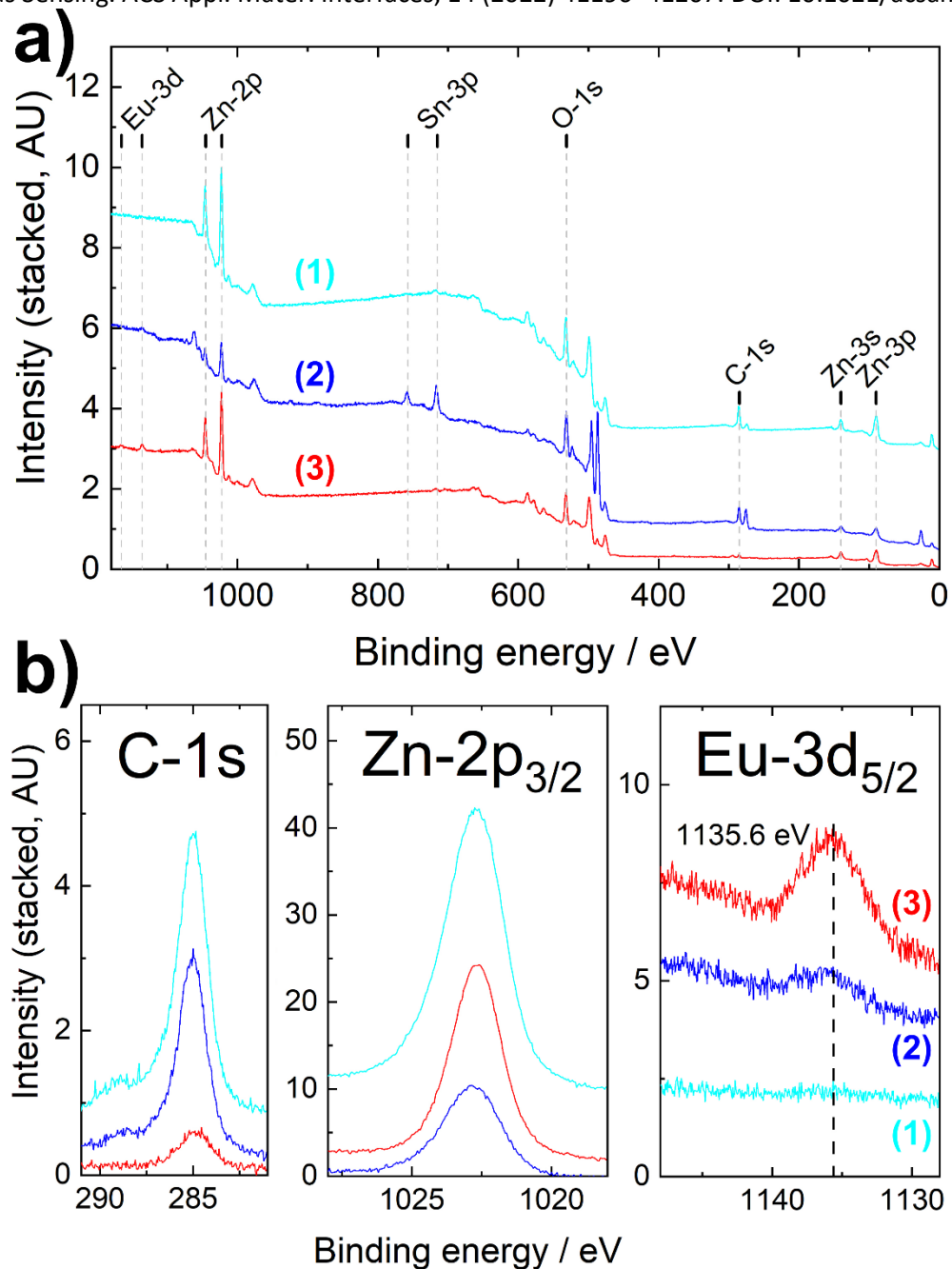


Figure 4. XPS spectra of ZnO:Eu nanowire samples: (a) overview spectrum indicating the presence of Eu, Zn, O and C; (b) high resolution spectra of C-1s line, Zn-2p_{3/2} line and Eu-3d_{5/2} line. (1) 3 μ M; (2) 6 μ M; and (3) 10 μ M EuCl₃ content in the electrolyte.

Please cite this paper as : C. Lupan, N. Wolff, J. Drewes, H. Krüger, A. Vahl, T. Pauporté, O. Lupan, B. Viana, L. Kienle, F. Faupel, R. Adelung, S. Hansen, Nanosensors Based on a Single ZnO:Eu Nanowire for Hydrogen Gas Sensing. ACS Appl. Mater. Interfaces, 14 (2022) 41196–41207. DOI: 10.1021/acsami.2c10975

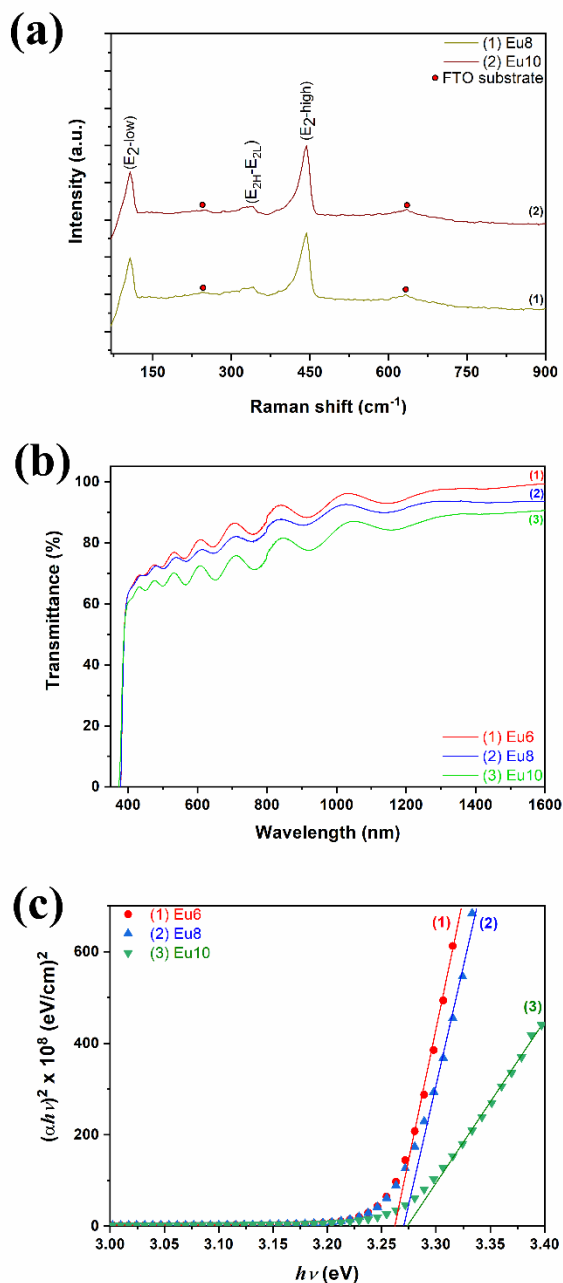


Figure 5. (a) Raman spectra of ZnO:Eu nanowires deposited with different Eu content: (1) 8 μM; and (2) 10 μM. (b) Transmission spectra of ZnO:Eu nanowires with different Eu content: (1) 6 μM; (2) 8 μM; and (3) 10 μM. (c) Plot of $(\alpha h\nu)^2$ vs $(h\nu)$ for ZnO:Eu nanowires with different Eu content: (1) 6 μM; (2) 8 μM and (3) 10 μM.

Please cite this paper as : C. Lupan, N. Wolff, J. Drewes, H. Krüger, A. Vahl, T. Pauporté, O. Lupan, B. Viana, L. Kienle, F. Faupel, R. Adelung, S. Hansen, Nanosensors Based on a Single ZnO:Eu Nanowire for Hydrogen Gas Sensing. ACS Appl. Mater. Interfaces, 14 (2022) 41196–41207. DOI: 10.1021/acsami.2c10975

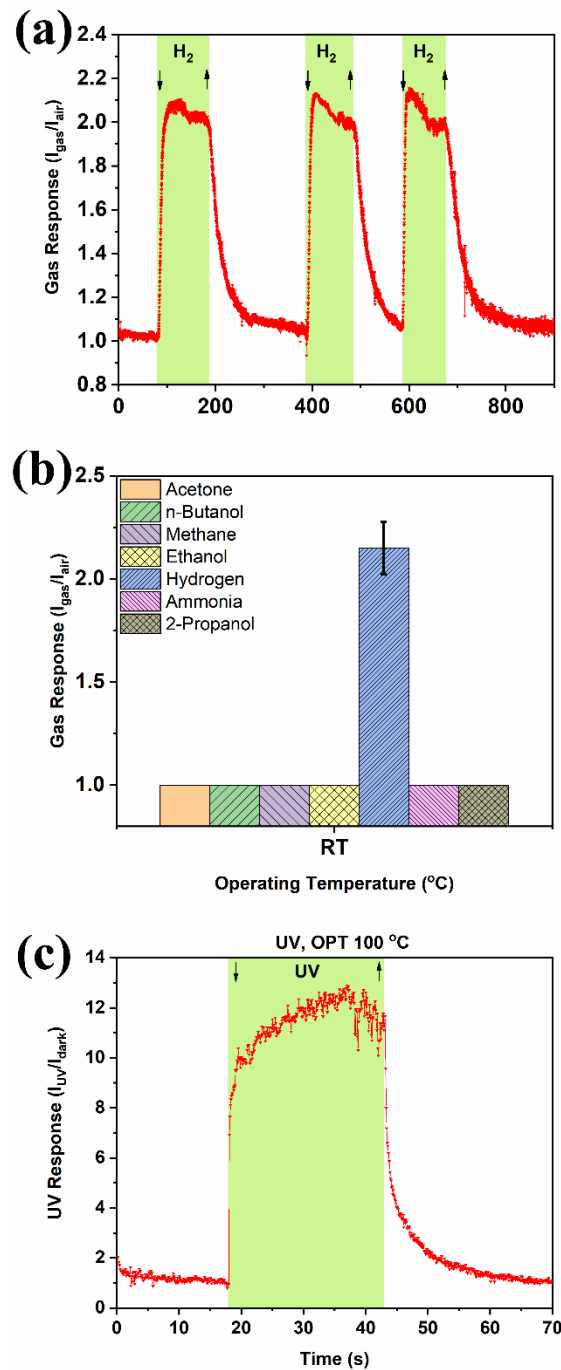


Figure 6. (a) Dynamic response of ZnO:Eu5 nanosensor to 100 ppm of hydrogen gas at room temperature. (b) Gas response of ZnO:Eu5 nanosensor to 100 ppm of various gases at room temperature. (c) UV response for ZnO:Eu5 nanosensor at 100 °C operating temperature.

Please cite this paper as : C. Lupan, N. Wolff, J. Drewes, H. Krüger, A. Vahl, T. Pauporté, O. Lupan, B. Viana, L. Kienle, F. Faupel, R. Adelung, S. Hansen, Nanosensors Based on a Single ZnO:Eu Nanowire for Hydrogen Gas Sensing. ACS Appl. Mater. Interfaces, 14 (2022) 41196–41207. DOI: 10.1021/acsami.2c10975

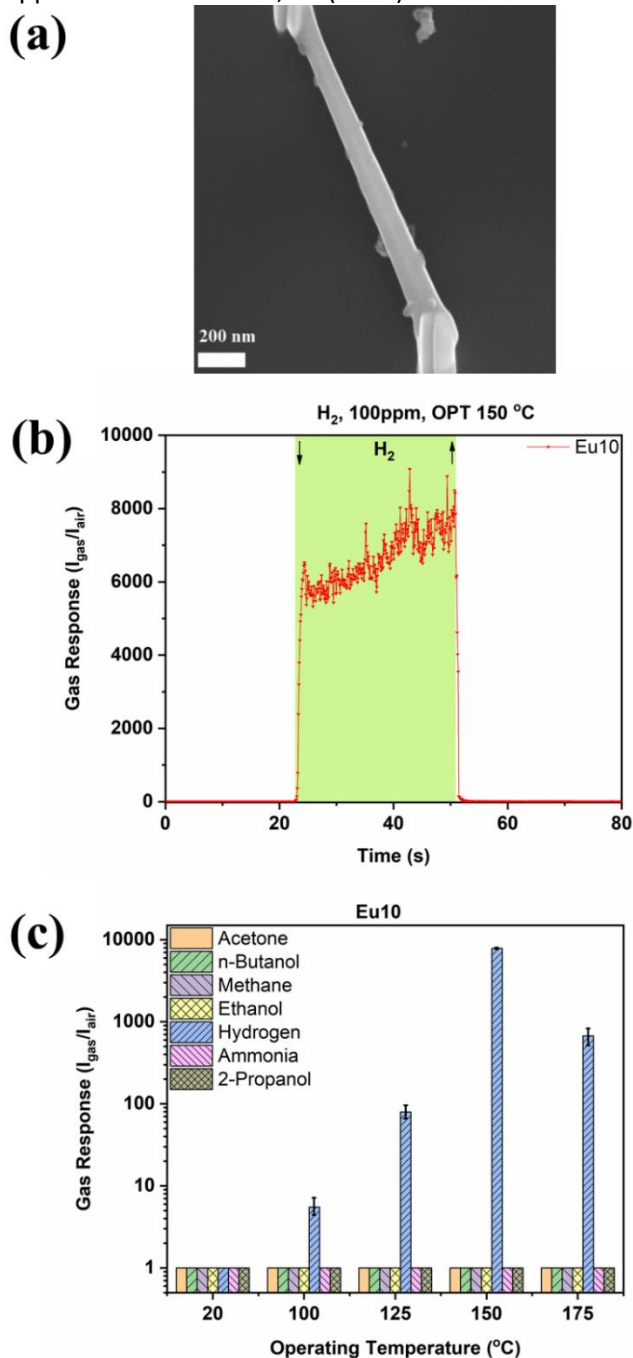


Figure 7. (a) SEM of sensor based on sample for ZnO:Eu10 (10 μ M EuCl₃ content in the electrolyte); (b) Gas response for 100 ppm hydrogen of a ZnO:Eu10 nanosensor at 150 °C operating temperature; (c) Gas response for 100 ppm of different gases at 20, 100, 125, 150 and 175 °C operating temperature for ZnO:Eu10 nanosensor.

Please cite this paper as : C. Lupan, N. Wolff, J. Drewes, H. Krüger, A. Vahl, T. Pauporté, O. Lupan, B. Viana, L. Kienle, F. Faupel, R. Adelung, S. Hansen, Nanosensors Based on a Single ZnO:Eu Nanowire for Hydrogen Gas Sensing. ACS Appl. Mater. Interfaces, 14 (2022) 41196–41207. DOI: 10.1021/acsami.2c10975

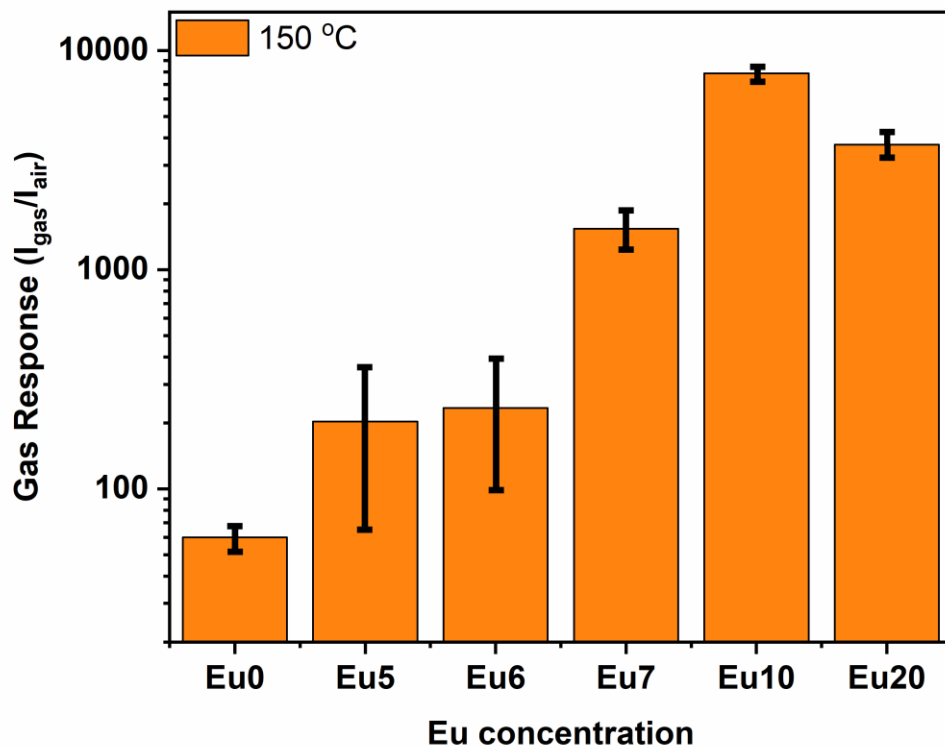


Figure 8. Gas response for 100 ppm hydrogen at 150 °C operating temperature for ZnO:Eu nanowires with different Eu content: (1) 0 μM ; (2) 5 μM ; (3) 6 μM ; (4) 7 μM ; (5) 10 μM ; and (6) 20 μM EuCl_3 concentration in the electrolyte.

Please cite this paper as : C. Lupan, N. Wolff, J. Drewes, H. Krüger, A. Vahl, T. Pauporté, O. Lupan, B. Viana, L. Kienle, F. Faupel, R. Adelung, S. Hansen, Nanosensors Based on a Single ZnO:Eu Nanowire for Hydrogen Gas Sensing. ACS Appl. Mater. Interfaces, 14 (2022) 41196–41207. DOI: 10.1021/acsami.2c10975

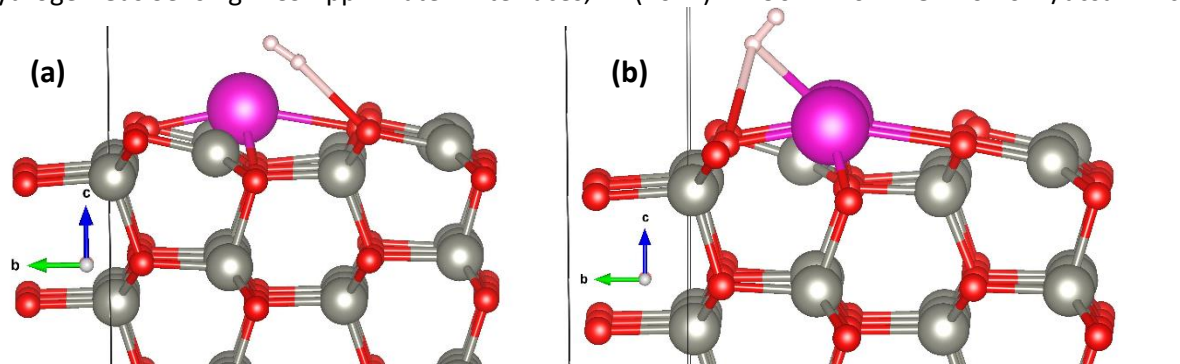


Figure 9. DFT relaxed structure of one H₂ molecule at (a) the Eu:ZnO(10 $\bar{1}$ 0) surface, and (b) the Eu₂:ZnO(10 $\bar{1}$ 0) surface. O, Zn, and Eu atoms are denoted by red, grey, and purple colors balls respectively, while small pink color balls denote H atoms.

Please cite this paper as : C. Lupan, N. Wolff, J. Drewes, H. Krüger, A. Vahl, T. Pauporté, O. Lupan, B. Viana, L. Kienle, F. Faupel, R. Adelung, S. Hansen, Nanosensors Based on a Single ZnO:Eu Nanowire for Hydrogen Gas Sensing. ACS Appl. Mater. Interfaces, 14 (2022) 41196–41207. DOI: 10.1021/acsami.2c10975

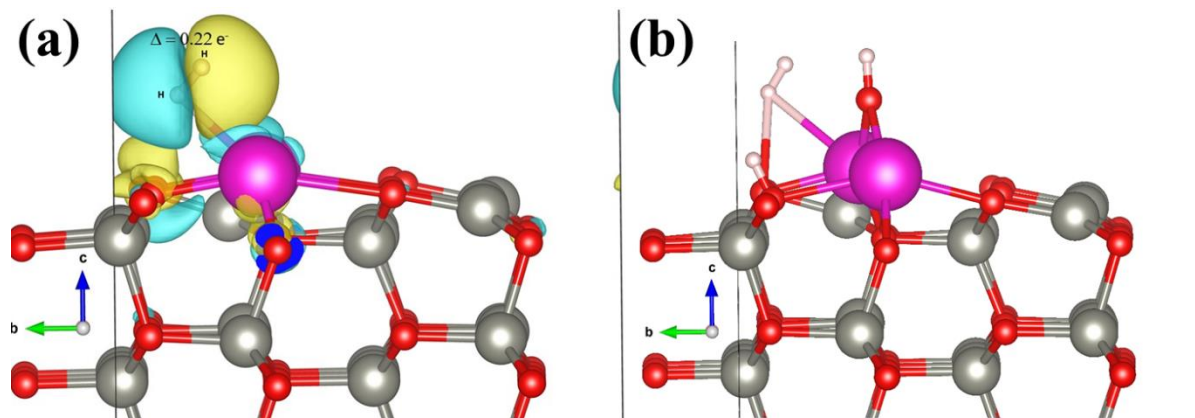


Figure 10. (a) Charge density difference plot iso-surfaces of the H₂ molecule interaction at the Eu₂:ZnO (10 $\bar{1}$ 0) surface, where the H₂ molecule gains 0.22 e⁻ in Bader charge. Blue and yellow colored iso-surfaces indicate negative and positive changes in charges, respectively. (b) H₂O and H₂ molecules over Eu₂:ZnO (10 $\bar{1}$ 0) surface